# An Explorative Study on Dye-Sensitized Solar Cells: Design, Fabrication and Comparative Performance Analysis

*A THESIS SUBMITTED TOWARDS PARTIAL FULFILMENT OF THE REQUIREMENTS FOR THE DEGREE OF*

**Master of Technology**
In
**Energy Science and Technology**

Course Affiliated To
**Faculty of Engineering and Technology**

Under

**Faculty Council of Interdisciplinary Studies**

**Law & Management**

**Jadavpur University**

**Submitted By**
## ARNAB JYOTI MANDAL

**Examination Roll No: M4ENR23006**
**Registration No: 160456 of 2021-2022**

**Under The Guidance Of**

## Dr. RATAN MANDAL
**Supervisor, Professor, and Director**

School of Energy Studies
Jadavpur University
Kolkata–700032
India
**2023**

**Master of Technology in Energy Science & Technology**
Course affiliated to
**Faculty of Engineering &Technology**
Under
**Faculty Council of Interdisciplinary Studies**
**Law & Management, Jadavpur University**
**Kolkata, India**

---

# CERTIFICATE OF RECOMMENDATION

This is to certify that the thesis entitled "**An Explorative Study on Dye-Sensitized Solar Cells: Design, Fabrication and Comparative Performance Analysis** " is a bonafide work carried out by **Mr. Arnab Jyoti Mandal** under our supervision and guidance for partial fulfillment of the requirements for the Post Graduate Degree of Master of Technology in Energy Science and Technology, during the academic session 2021-2023.

---

**THESIS SUPERVISOR**
**Dr. RATAN MANDAL**
Director and Professor
School of Energy Studies
Jadavpur University
Kolkata–700032

---

**DEAN**
**Faculty Council of Interdisciplinary Studies,**
**Law and Management**
Jadavpur University
Kolkata–700032

**Master of Technology in Energy Science & Technology**
Course affiliated to
**Faculty of Engineering &Technology**
Under
**Faculty Council of Interdisciplinary Studies**
**Law & Management, Jadavpur University**
**Kolkata, India**

---

# CERTIFICATE OF APPROVAL

This foregoing thesis is hereby approved as a credible study of an engineering subject carried out and presented in a manner satisfactory to warranty its acceptance as a prerequisite to the degree for which it has been submitted. It is understood that by this approval the undersigned does not endorse or approve any statement made or opinion expressed or conclusion drawn therein but approves the thesis only for the purpose for which it has been submitted**.**

**Committee of** ----------

**The final examination for** ----------

**Evaluation of Thesis** ----------

# DECLARATION OF ORIGINALITY AND COMPLIANCE OF ACADEMIC ETHICS

I hereby declare that this thesis contains a literature survey and original research work by the undersigned candidate, as part of his Master of Technology in Energy Science and Technology studies during the academic session 2021-2023.

All information in this document has been obtained and presented in accordance with academic rules and ethical conduct.

I also declare that, as required by these rules and conduct, I have fully cited and referred all materials and results that are not original to this work.

| | | |
|---|---|---|
| **Name** | **:** | **Arnab Jyoti Mandal** |
| **Examination Roll No.** | **:** | **M4ENR23006** |
| **Thesis Title** | **:** | **An Explorative Study on Dye-Sensitized Solar Cells: Design, Fabrication and Comparative Performance Analysis** |
| **Signature** | **:** | |
| **Date** | **:** | |

# ACKNOWLEDGEMENTS

I feel honored to express my deepest respect, reverence, indebtedness, and heartiest gratitude to my respected supervisor Prof. Ratan Mandal (Director, School of Energy Studies, Jadavpur University) for his acute interest in every detail of this project, judicious guidance, constant inspiration and help during the entire period of execution of the present project work.

I am also grateful to Dr. Tushar Jash (Professor, School of Energy Studies, Jadavpur University) and Deepanjan Majumder, Tarak Nath Chell for their valuable advice and encouragement during the period of the project work.

I am also grateful to all my classmates for their constant motivation and assistance during the project.

Finally, I want to thank my parents who have supported me in every ups and downs of my life and have always encouraged me without expecting anything in return.

---

**ARNAB JYOTI MANDAL**
**School of Energy Studies**
**Jadavpur University**
**Kolkata–70003**

# Contents

# List of Figures

# List of Tables

# Chapter-1
# Introduction

## 1.1 Energy Scenarios in India

India plays a significant role in the global energy economy, experiencing a substantial increase in energy consumption since 2000. As compared to other countries India ranks third following the United States (Figure 1.1 [1]). This surge can be attributed to factors such as a growing population, poised to become the world's largest, and rapid economic growth. Achieving near-universal household access to electricity in 2019 indicates significant progress, with over 900 million individuals gaining electrical connections within two decades. India's ongoing industrialization globally based on per energy consumption as shown in Figure 1.2 [1] and urbanization processes will exert significant pressure on the energy sector and policymakers, which includes electricity, transport, heating, and cooking, consumption in India remains below half of the global average, and variations exist in energy usage and service quality between different states as well as rural and urban areas. Ensuring affordability and reliability of energy supply are critical concerns for Indian consumers [2].

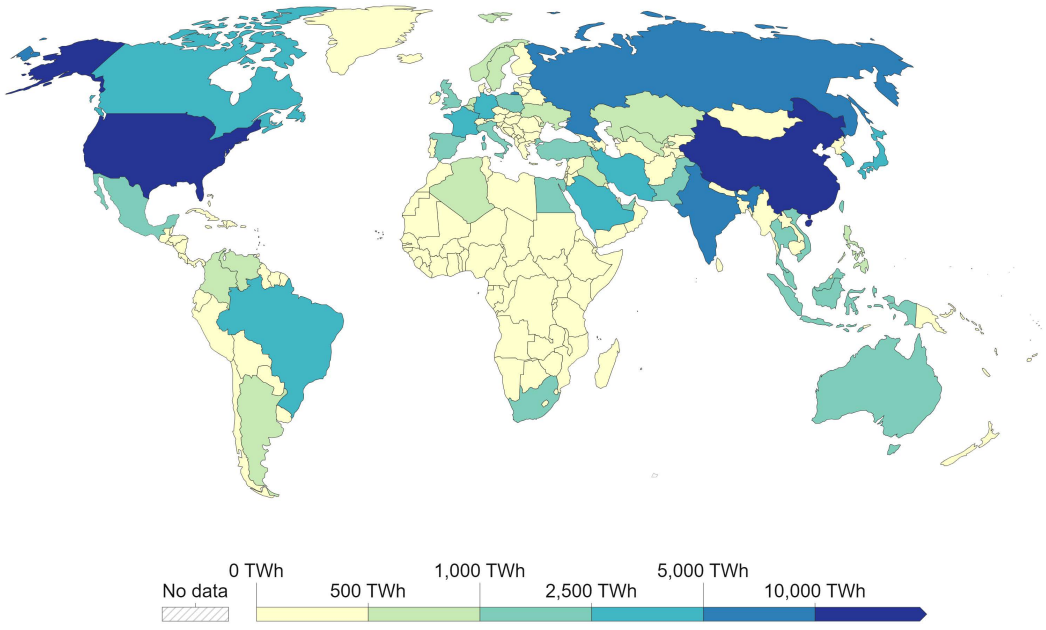


Figure 1.1 Total Energy (Mtoe) Consumption 2021

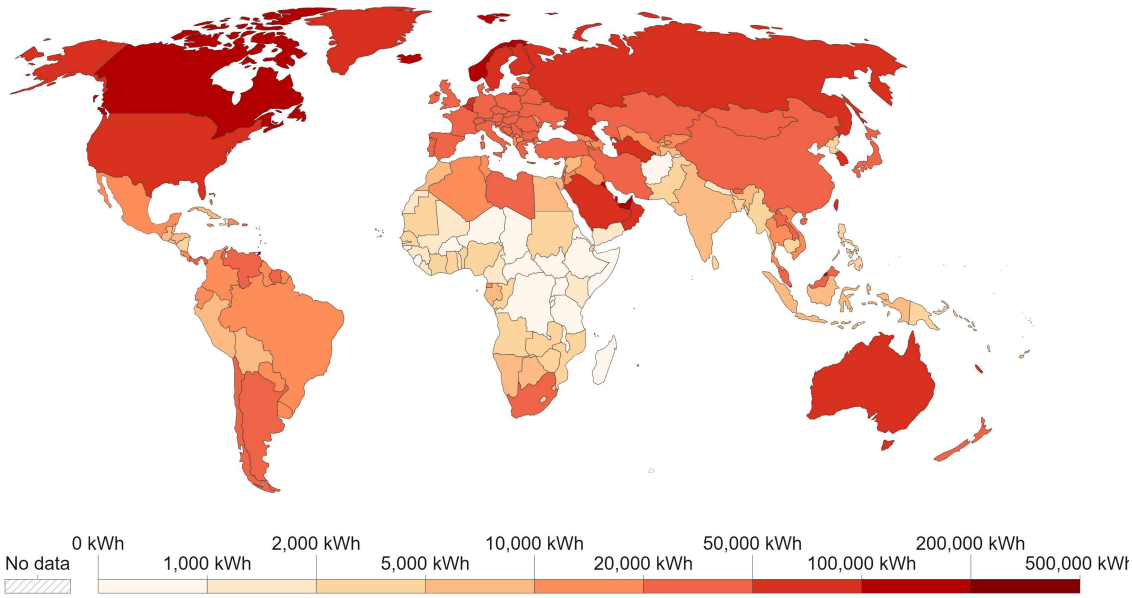


Figure 1.2 Energy consumption per capita 2021

Energy scenarios in India can be broadly categorized into three main aspects: the current energy mix, future projections, and policy directions. Let's explore each of these scenarios:

## 1.2 Current Energy Mix

India's current energy mix is characterized by a significant reliance on fossil fuels, particularly coal, as well as a growing contribution from renewable energy sources. However, the specific composition varies across sectors. Some key features of the current energy mix include:

- Electricity Generation: Currently, the majority of electricity production in India is heavily reliant on coal-based thermal power plants; accounting for approximately, 75% of the country's total power generation [3]. Coal-based thermal power plants dominate India's electricity generation, accounting for a substantial portion of the energy mix. In India installed capacity and expected capacity of electricity is given in Figure 1.3 [4]. However, the gross generation (Figure 1.3) with the share of renewable energy, expected gross generation will be reduced by 50% [4].

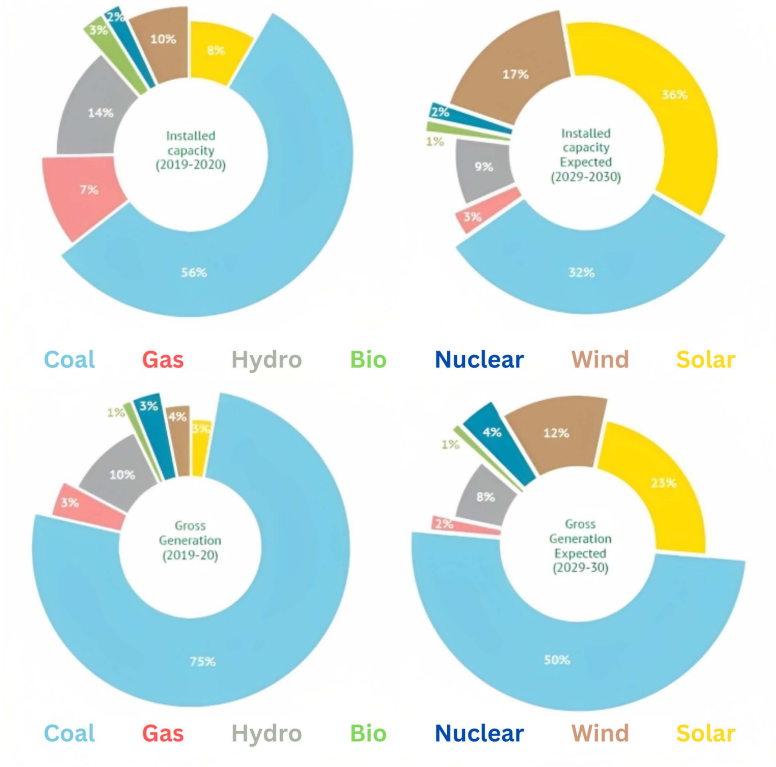


Figure 1.3 Installed capacity vs Gross power generation in India

- Transportation: The transportation sector heavily depends on petroleum-based fuels, primarily petrol, and diesel, for various modes of transport. However, the government is promoting the adoption of electric vehicles (EVs) to reduce dependence on fossil fuels and curb emissions [5].

- Cooking and Heating: In rural areas, traditional biomass sources such as firewood and agricultural residues are commonly used for cooking and heating purposes. However, there is a gradual shift towards cleaner cooking alternatives such as LPG and electricity [6].

## 1.3 Future Projections

India has set ambitious targets and aspirations for its future energy mix, driven by the need for sustainable development, energy security, and climate change mitigation. Some of the key projections for India's energy scenario include:

- Renewable Energy Expansion: India aims to significantly increase the share of renewable energy in its overall energy mix. The targets include achieving almost 500 GW (Figure 1.4 [7]) of renewable energy capacity by 2030 [8], with a focus on solar and wind power. This expansion aims to reduce carbon emissions, enhance energy security, and promote decentralized energy generation.

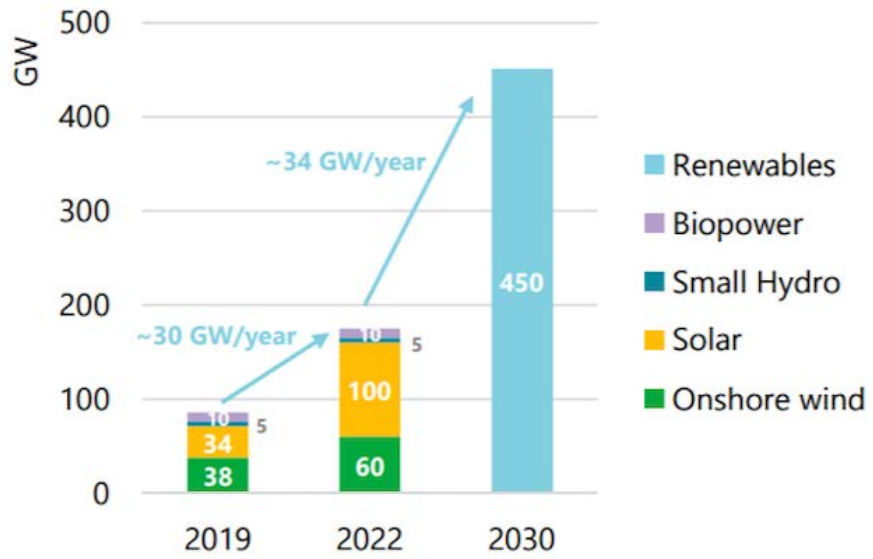


Figure 1.4 Installed Capacity in 2019 relative to 2022 & 2023 targets in India

- Energy Efficiency: Improving energy efficiency across sectors is a crucial aspect of India's future energy scenario. Various initiatives and policies are being implemented to promote energy-efficient technologies and practices, particularly in industries, buildings, and appliances [9].

- Electric Mobility: The government has set a vision to transition to electric mobility by promoting the adoption of electric vehicles and establishing a robust charging infrastructure network. The aim is to reduce the reliance on petroleum-based fuels, lower vehicular emissions, and improve air quality [10].

## 1.4 Policy Directions

The Indian government has implemented several policies and initiatives to shape the energy scenario in the country. These policies aim to address various challenges, promote renewable energy, enhance energy efficiency, and ensure energy security. Some notable policy directions include:

- National Solar Mission: The Jawaharlal Nehru National Solar Mission aims to promote the deployment of solar power and achieve grid parity by supporting solar power projects, facilitating research and development, and encouraging domestic manufacturing of solar equipment [11].

- UJALA (Unnat Jyoti by Affordable LEDs for All): This program focuses on promoting energy-efficient LED lighting across the country by providing LED bulbs at subsidized rates, thereby reducing electricity consumption and costs [12].

- Pradhan Mantri Ujjwala Yojana: This scheme aims to provide clean cooking fuel connections to households below the poverty line, thereby reducing the dependence on traditional biomass for cooking and improving indoor air quality [13].

- Energy Conservation Building Code (ECBC): The ECBC sets energy efficiency standards for commercial buildings, promoting the use of energy-efficient building materials, lighting, and cooling systems [14].

These policy directions, along with technological advancements, international collaborations, and public participation, play a crucial role in shaping India's energy scenarios toward a cleaner, more sustainable, and more resilient future.

## 1.5 Energy Demand in India

As per World Energy Outlook 2021 of IEA, the current share of India in global primary energy consumption is 6.1% and is likely to increase to about 9.8% understated policy scenario by 2050 [15]. India has been experiencing rapid economic growth, resulting in increased industrialization, commercial activities, and infrastructure development. Sector-wise electricity consumption is provided in this pie chart (Figure 1.5 [16]). These developments require substantial energy inputs, leading to a rise in energy demand.

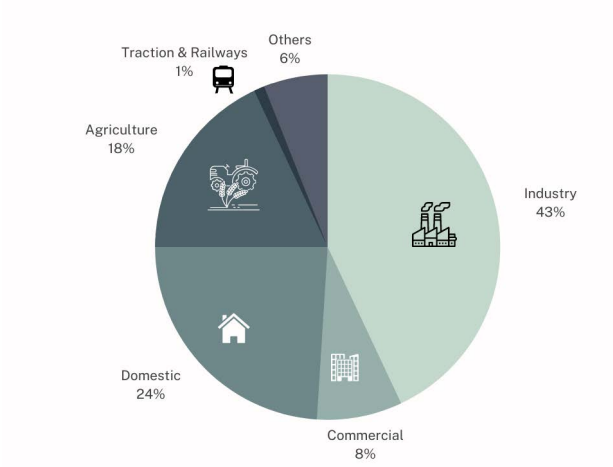


Figure 1.5 Sector-wise Electricity Consumption in India

According to recent data released by the United Nations, India is on track to surpass China and become the world's most populous country by the middle of this year. The population projections indicate a significant demographic shift, with India taking the lead in terms of total population size[17]. Different energy sectors of India will be affected which include:

### 1.5.1 Residential Sector

The residential sector accounts for a significant portion of energy demand in India. This includes electricity consumption for lighting, cooking, space heating, and cooling, as well as energy use for water heating and other household appliances (Figure 1.6 [18]). The demand for energy in this sector is influenced by population growth, urbanization, and improvements in living standards.

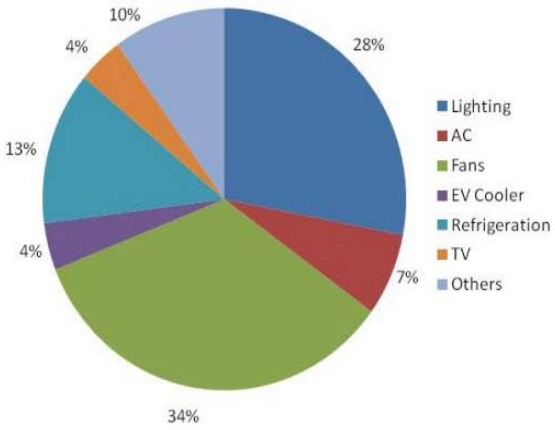


Figure 1.6 Energy Consumption in Residential Buildings in India

## 1.5.2 Commercial Sector

The commercial sector comprises establishments such as offices, shopping malls, hotels, and hospitals. Energy demand in this sector is driven by lighting, air conditioning, heating, ventilation, and other electrical and electronic equipment used for commercial activities as shown in Figure 1.7 [18]. The growth of the service sector and increasing commercial activities contribute to the rising energy demand in this sector.

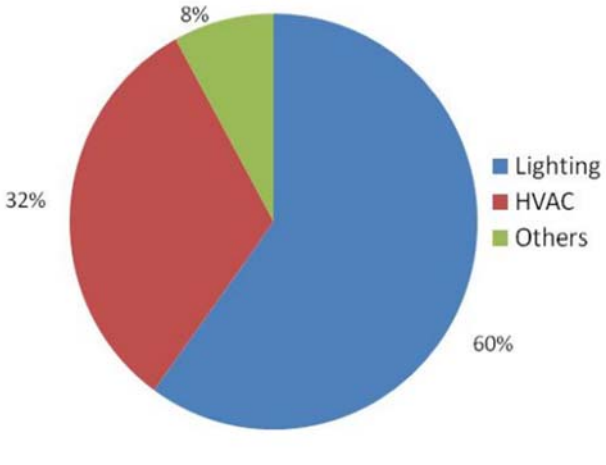


Figure 1.7 Energy Consumption in Commercial Buildings in India

## 1.5.3 Industrial Sector

The industrial sector is a major consumer of energy in India. Energy demand in this sector arises from manufacturing processes, machinery operations, and other industrial activities. Industries such as steel, cement, chemicals, textiles, and food processing require significant amounts of energy for production and operation. In Figure 1.8 [19] the various sector's contribution is reflected. Industrialization and economic growth contribute to the increasing energy demand in this sector.

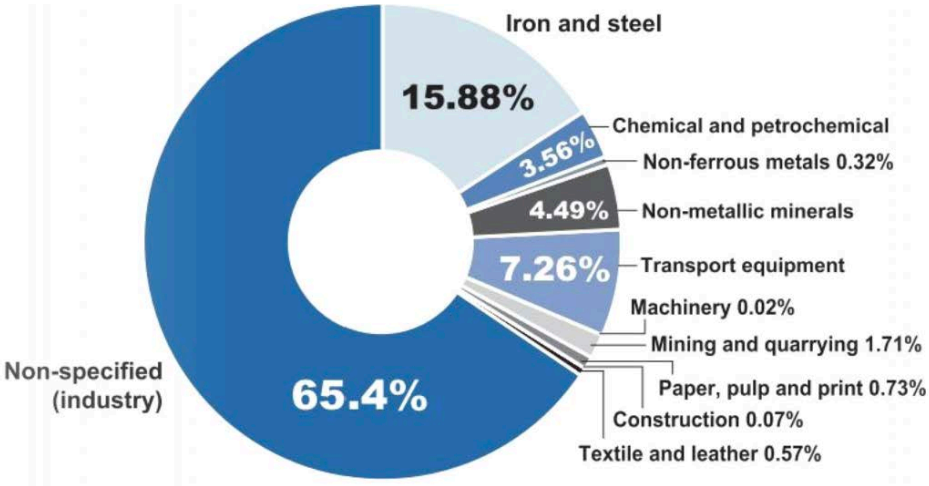


Figure 1.8 Industrial Sector Energy Consumption

## 1.5.4 Transportation Sector

The transportation sector encompasses various modes of transport, including road, rail, air, and waterways. Energy demand in this sector primarily arises from the consumption of fossil fuels, such as petrol, diesel, and aviation fuel. Population growth, urbanization, increasing vehicle ownership, and the movement of goods and people drive the demand for transportation energy [20].

## 1.5.5 Agricultural Sector

The agricultural sector is a crucial part of India's economy. Energy demand in this sector is mainly related to irrigation, agricultural machinery, and post-harvest processing. Irrigation pumps, tractors, and other machinery require energy, often in the form of electricity or

diesel. As agricultural practices become more mechanized and efficient, the demand for energy in this sector increases [21].

Understanding the sector-wise energy demand is essential for policymakers and energy planners to develop strategies and policies that address the specific requirements and challenges of each sector. It also helps in identifying opportunities for energy efficiency improvements, renewable energy integration, and sustainable development practices.

## 1.6 Solar Energy in India

India, with a population of 1.3 billion, has a substantial energy demand to support its fast-growing economy. Over the past seven decades, efforts have been made to transform India from a power-deficit nation to one that is energy-independent. Presently, India has achieved a surplus in power generation, boasting an installed electricity capacity of over four lacks MW [22].

In line with the goal of sustainable development, India is actively transitioning its power generation mix towards a greater reliance on renewable energy sources. The country now stands as the world's fourth largest producer of renewable energy [23], with non-fossil fuel sources contributing 40% to its total installed electricity capacity. Solar energy holds several advantages that make it a favorable choice for implementation in India compared to other renewable energy resources. Here are some reasons why solar energy is well-suited for India:

### 1.6.1 Abundant Solar Resource

India receives abundant sunlight throughout the year due to its geographical location. The country has vast solar potential, especially in regions with high solar insolation levels. This makes solar energy a reliable and readily available resource for electricity generation .

## 1.6.2 Energy Security and Independence

Solar energy offers the advantage of reducing India's dependence on fossil fuel imports. As per World Bank Report (Figure 1.9 [24]), the potential for India by harnessing solar power domestically, can enhance its energy security and reduce vulnerability to fluctuations in international fuel prices.

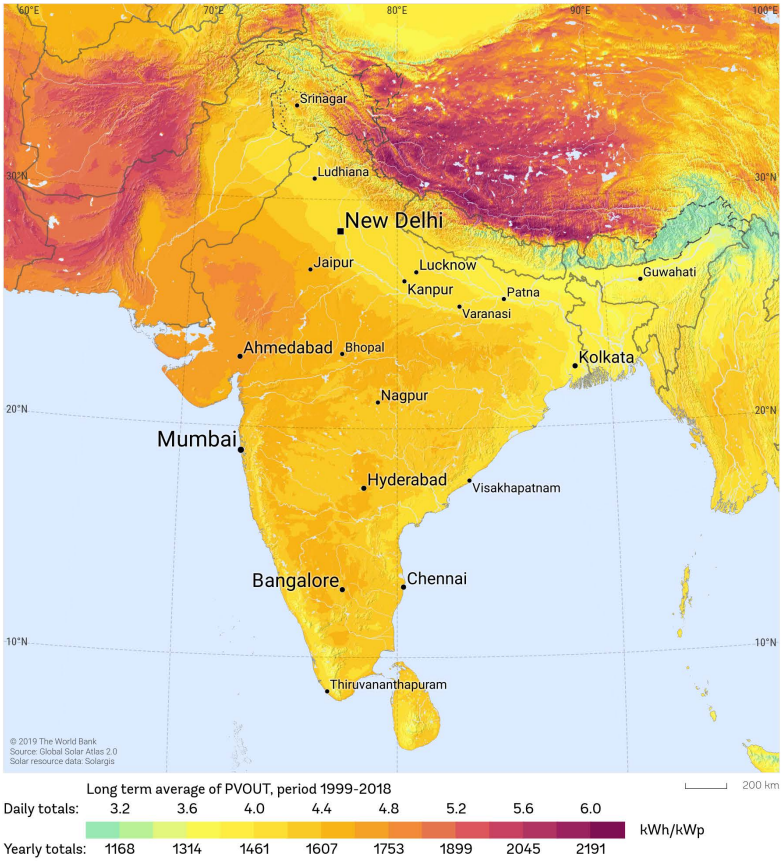


Figure 1.9 SPV Power Potential in India

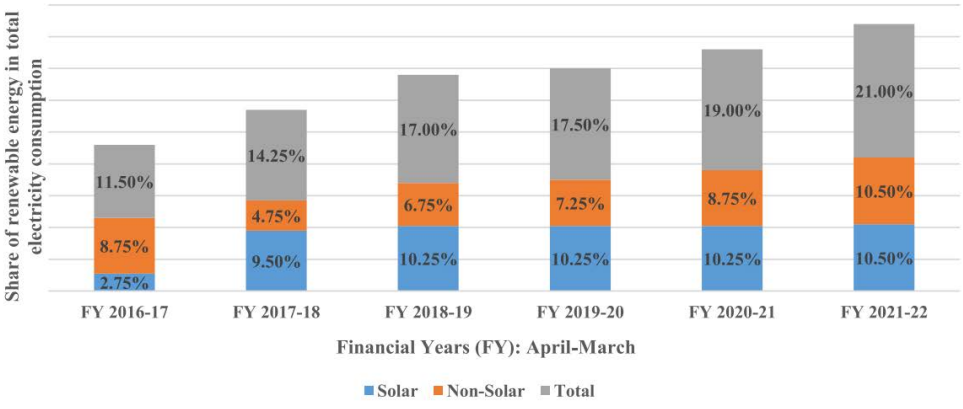


Figure 1.10 Percentage share of renewable energy consumption in India

## 1.6.3 Scalability and Modularity

The share of renewable energy is increasing yearly ( Figure 1.10 [25]). In terms of installed capacity, solar power is expected to expand to over 740 GW by 2040, compared to about 220 GW for coal-fired power, an increase of about 3.4 times compared to 2020 (Figure 1.11 [26]). As of 30th November 2022, the Ministry of New and Renewable Energy (MNRE) in India reported that the photovoltaic capacity has reached 61.97 GW [27]. Solar energy projects can be easily scaled up or down to meet diverse energy demands, making it a flexible solution for various applications. Solar power plants can range from small-scale rooftop installations to large-scale solar parks, providing options for decentralized energy generation and rural electrification.

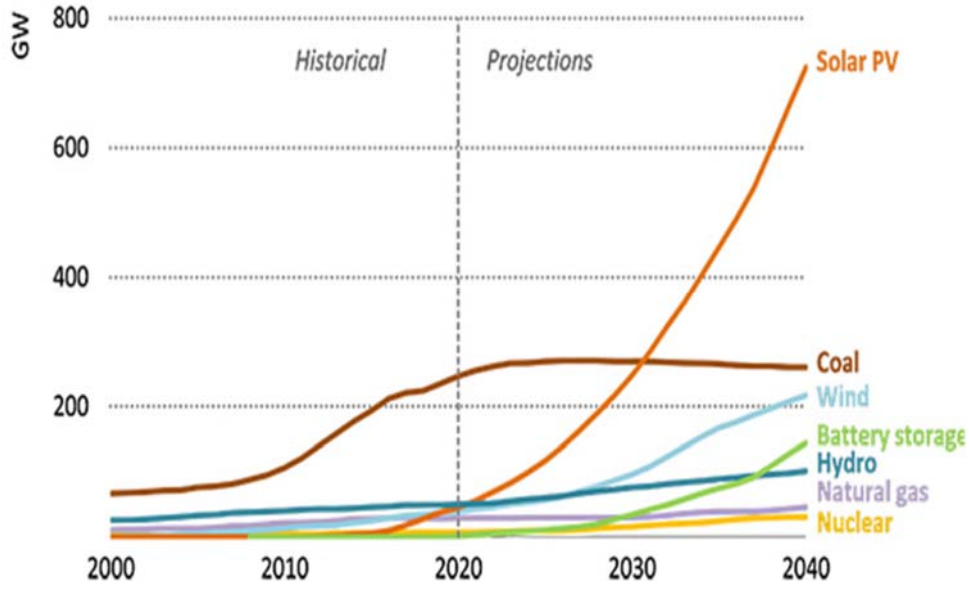


Figure 1.11 Renewable Energy Targets of India

## 1.6.4 Environmental Benefits

Solar energy is a clean and renewable energy source that produces minimal greenhouse gas emissions and has a significantly lower environmental impact compared to fossil fuels (Figure 1.12 [28]). Adopting solar energy helps India in mitigating climate change, reducing air pollution, and protecting the environment.

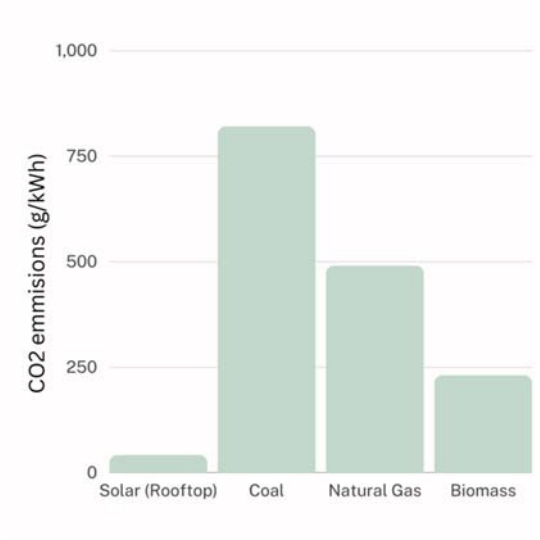


Figure 1.12 $CO_2$ emissions from different sources [Source: IPCC]

## 1.6.5 Cost Competitiveness

The cost of solar energy has been declining rapidly in recent years (Figure 1.13 [29]), making it increasingly cost-competitive with conventional sources of electricity. The falling prices of solar panels and technological advancements have made solar energy economically viable, especially when compared to fossil fuel-based power generation.

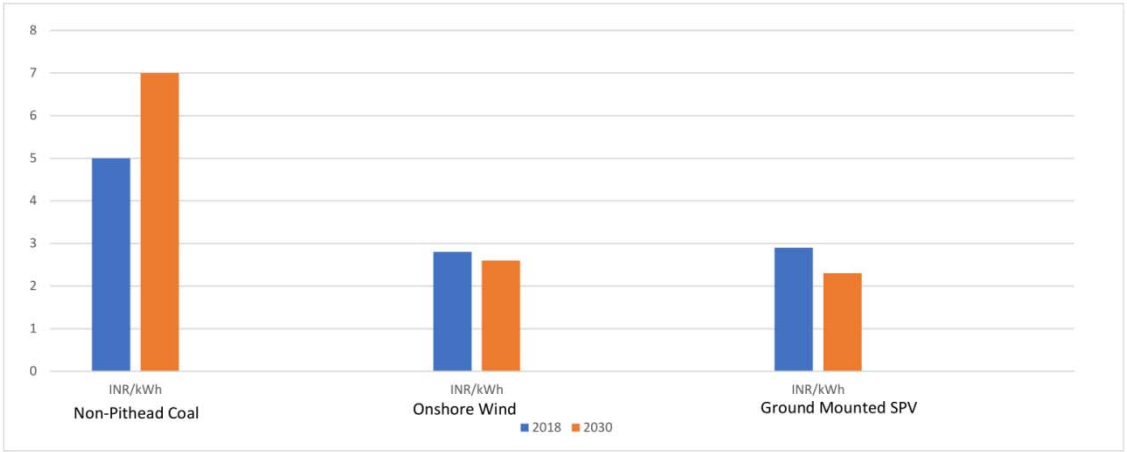


Figure 1.13 Energy Generation Costs in India [Source: TERI]

## 1.6.6 Government Support and Policy Framework

The Indian government has been actively promoting solar capacity (MW) (Figure 1.14 [30]) in various sectors through initiatives and policies. Schemes such as the National Solar Mission and incentives for solar power development have created a favorable environment for solar energy implementation. This support has facilitated the growth of the solar industry in India.

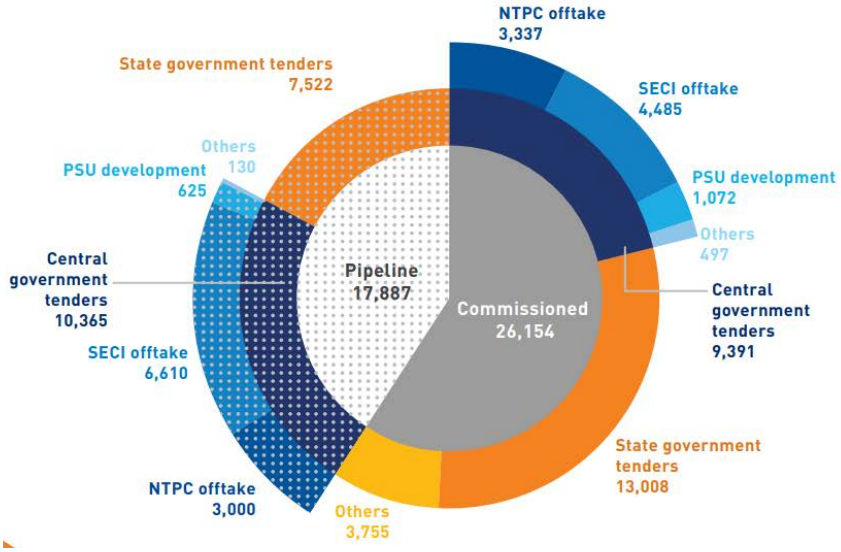


Figure 1.14 Total utility scale solar capacity in MW as on March, 2019

Considering these factors, solar energy emerges as a compelling choice for India, offering a clean, abundant, and domestically available resource that can contribute significantly to the country's energy security, economic growth, and environmental sustainability.

# 1.7 Justification for Research on Dye-Sensitized Solar Cells

In today's dynamic political and economic landscape, it is clear that no single photovoltaic technology can fulfill the diverse demands of every application. However, as different photovoltaic technologies continue to advance in efficiency and commercial viability, it becomes crucial for companies to identify their unique niche. While dye-sensitized solar cells (DSSCs) may not surpass conventional silicon technologies in terms of photovoltaic

efficiency or be suitable for large-scale energy collection in expansive solar fields, they possess distinct advantages and potential that make them well-suited for a specific niche in the photovoltaic industry. The global market of DSSCs has grown yearly (Figure 1.15) [31]. One significant advantage of DSSCs lies in their low materials and processing costs. This cost-effectiveness positions them favorably for integration into consumer goods. By leveraging their affordability, DSSCs have the potential to revolutionize the way we power everyday products, such as portable electronic devices or wearable technology. Their application in these consumer goods can provide renewable energy solutions to a wider audience, contributing to sustainability efforts on a smaller scale [32].

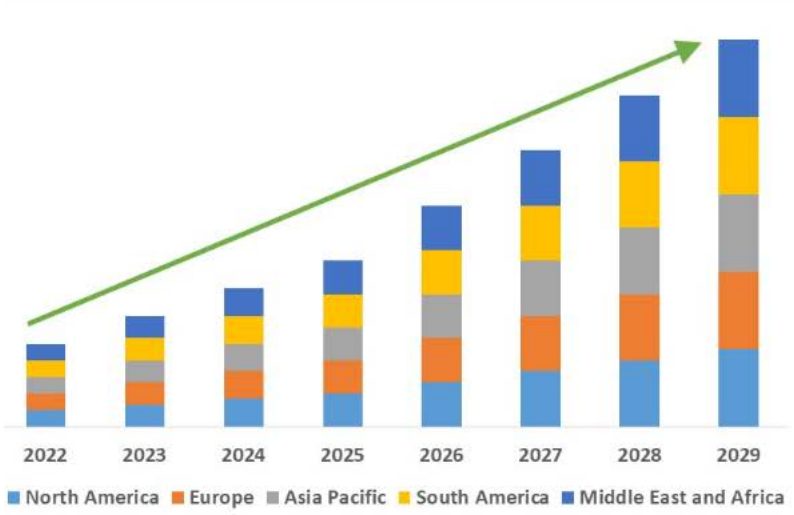


Figure 1.15 Globally Dye Sensitized Solar Cells expected market size.

Another noteworthy characteristic of DSSCs is their relatively higher efficiency when exposed to lower-intensity light. This attribute suggests potential utilization in indoor environments. By harnessing ambient light sources within buildings, DSSCs could serve as an efficient energy-harvesting solution for powering various indoor applications. Such applications might include wireless sensors, smart home devices, or low-power electronic systems that operate in indoor settings. As shown here in Figure 15 [31], the global market of DSSCs is increasing, there are some key points behind the growing market. The research on Dye-Sensitized Solar Cells (DSSCs) is driven by several factors, including the available range of materials and their environmental impact, particularly in comparison to other solar cell technologies.

DSSCs offer the advantage of utilizing a wide range of materials for their construction. Unlike traditional silicon-based solar cells, DSSCs can incorporate various organic and inorganic dyes, as well as alternative electrode and electrolyte materials. This flexibility allows researchers to explore and optimize different material combinations to achieve higher efficiency and performance. Another important factor driving research on DSSCs is their reduced environmental impact compared to other solar cell technologies. DSSCs have the potential to be more environmentally friendly due to their lower energy and resource requirements during manufacturing. Additionally, the ability to use non-toxic and abundant materials in DSSCs, such as certain organic dyes and alternative electrolytes, reduces the environmental footprint of the technology.

DSSCs have the advantage of employing materials that are generally less toxic compared to some other solar cell technologies including conventional technologies. For example, the electrolytes used in DSSCs can be based on organic solvents instead of toxic heavy metals, such as cadmium or lead. This reduced toxicity not only improves the safety aspects during production and operation but also offers potential benefits in end-of-life disposal and recycling.

Considering the available range of materials and the reduced environmental impact with less toxicity, DSSCs hold promise as sustainable and environmentally friendly solar cell technology. By researching DSSCs, scientists and engineers aim to further optimize the performance, efficiency, and stability of these cells, ultimately contributing to the development of cleaner and more sustainable energy sources.

## 1.8 Objectives of the Thesis

Objectives of this explorative study is to investigate and analyze the design, fabrication, and comparative performance of alternative dye-based solar cells in the context of Dye Sensitized Solar Cells. The research will involve designing and fabricating DSSCs with different alternative dyes by evaluating their performance in terms of power conversion efficiency. Comparative analysis will be conducted to assess the advantages and limitations of each dye in terms of its light absorption capabilities, materials properties, and electrical parameter characteristics.

Furthermore, the study will investigate the influence of different fabrication techniques, such as various electrode materials and electrolytes, on the overall performance of alternative dye-based DSSCs. By examining these factors, the aim is to identify the optimal combination of dye, electrode, and electrolyte materials that can enhance the efficiency and stability of DSSCs.

To achieve the goal of our thesis, it is essential to conduct a comprehensive and meticulous review of existing literature. That has enabled us to gain a thorough understanding of the techniques employed by previous researchers and extract key insights that assisted us in accomplishing our objective. The findings of this research contribute to a deeper understanding of the potential of alternative dyes, offering valuable insights for the development of Dye Sensitized Solar Cells technologies.

## 1.9 Conclusion

India's role in the global energy economy is significant and has experienced a substantial increase in energy consumption over the past two decades. This surge can be attributed to factors such as a growing population and rapid economic growth. While India has made significant progress in achieving near-universal household access to electricity, challenges remain in ensuring the affordability and reliability of energy supply. India's current energy mix is characterized by a heavy reliance on coal-based thermal power plants for electricity generation, petroleum-based fuels for transportation, and traditional biomass for cooking and heating in rural areas. However, there is a growing contribution from renewable energy sources, and the government has set ambitious targets for their expansion, including a focus on solar and wind power.

We must keep in mind that no single photovoltaic technology can cater to all applications in the current political and economic climate, DSSCs offer a unique niche. Their cost-effectiveness and potential integration with consumer goods make them suitable for powering everyday products. In conclusion, the introduction serves as the gateway to the research topic, providing a brief overview of the study's purpose, objectives, and significance. To fulfill the objectives, the literature review critically examined in the next chapter, existing scholarly works to establish the research gap and theoretical foundation for the study. Together, these sections lay the foundation for the research by setting the context, highlighting the knowledge deficit, and justifying the need for further investigation.

# Chapter-2
# Literature Review

Chapter 1 provides insight into the escalating need for energy and the continuously increasing energy demand. To safeguard the environment, it becomes imperative to transition from conventional energy sources to renewable alternatives. Among the array of renewable energy sources, solar energy emerges as a prominent contender due to its inherent advantages. Consequently, directing our attention towards solar energy and the materials employed in solar cells becomes crucial for a better future.

In Chapter 2, we delve into the stages of previous noteworthy endeavors conducted worldwide. By examining these earlier initiatives, we gain valuable knowledge, leading us to recognize the immense potential of dye-sensitized solar cells (DSSCs) as a pivotal member of the solar cell family. DSSCs are poised to compete with conventional silicon solar cells in the forthcoming era.

Solar energy can undergo conversion into different energy forms, including chemical energy, bioenergy, electricity, or heat. In the context of this research, our focus lies on the photovoltaic (PV) conversion method. The photovoltaic device, commonly known as a solar cell, comprises two essential components, namely the cathode and anode. It is worth noting that the discovery of the photovoltaic effect can be attributed to Edmon Becquerel in the year 1839 [33]. After almost several decades, Charles introduced the initial solar cell, crafted from selenium and gold, exhibiting an approximate photon-to-electricity conversion efficiency of 1%. Notwithstanding, it is important to acknowledge that Albert Einstein played a pivotal role as a pioneering theoretical researcher in the field of the photovoltaic effect [34].

Albert Einstein's significant contributions emphasized that electrons are emitted from materials as a result of photon absorption, establishing a fundamental understanding of the photovoltaic effect. Presently, the physics behind photovoltaic conversion in solar cell devices remains a topic that is not extensively elucidated. While silicon solar cells have achieved commercial viability within the photovoltaic market, there is a growing market share for less expensive semiconductor solar cells like CdTe, Cu(In, Ga)Se, and amorphous or crystalline thin silicon solar cells. Additionally, emerging types of PV devices such as organic solar cells and dye-sensitized solar cells, which encompass both organic and inorganic variants, hold great potential for the solar cell market.

## 2.1 History of Dye-Sensitized Solar Cells

Becquerel et al [35] utilized an electrode composed of a platinum sheet coated with a thin layer of silver chloride in 1839. While the exact nature of the second electrode is not explicitly mentioned in the account, likely, it was also a platinum sheet, immersed in a solution of electrolyte. When the silver chloride electrode was exposed to illumination, an electric current was generated. The scientist successfully demonstrated that this current was not a result of a heating effect, and to examine the spectral response, they employed color filters placed between the electrode and the light source, which happened to be the sun. By doing so, they obtained a rudimentary spectral response curve.

During the 1960s, H. Gerischer et al. [36] made a significant discovery regarding the generation of electricity at semiconductor electrodes through the illumination of light on an organic dye. This breakthrough revealed the capability of organic dyes to produce an electric current in electrochemical cells. In this study, the researchers aim to explore the potential of electrochemical methods in investigating sensitization effects on various semiconductor surfaces. To accomplish this, they selected two representative semiconductors: zinc oxide, which is an example of an n-type inorganic semiconductor, and perylene, a hydrocarbon that serves as a typical p-type organic semiconductor.

H. Tributsch et al. [37] investigated excited chlorophyll molecules at semiconductor electrodes, provides valuable insights into the underlying mechanisms of photosynthesis and offers potential applications in the field of renewable energy conversion. By further understanding the behavior of chlorophyll and its interactions with semiconductor materials, researchers can contribute to the development of innovative approaches for harnessing solar energy and improving the efficiency of energy conversion systems.

Michio Matsumura et al. [38] conducted a study in 1980 and discovered that the efficiency of dye molecules in dye-sensitized photocells could be enhanced by carefully adjusting the porosity of the semiconductor oxide material. However, they encountered a significant challenge concerning the stability of the dye in these systems. They achieved an apparent quantum efficiency of the photocurrent of up to 20% by dyeing a sintered ZnO electrode with rose bengal and immersing it in an electrolyte solution containing the I-/&- couple.

This efficiency was approximately one order of magnitude higher than previously achieved efficiencies. Additionally, they obtained a power conversion efficiency of 4 under monochromatic light with an intensity of 1.5%.

Grätzel et al. [39] first introduced the Dye-sensitized Solar Cells, also known as Grätzel cells, which are a type of thin-film solar cells that convert sunlight into electricity. They were first invented by Michael Grätzel and Brian O'Regan in 1988, showed improved conversion efficiency of 7.12% set a remark in the field of solar cells, and have since attracted significant attention due to their unique advantages compared to traditional silicon-based solar cells. DSSCs are based on a photoelectrochemical system in which a photosensitizer dye is used to absorb light and generate electrons, which are then transported through a mesoporous semiconductor film to an electrode, creating an electric current.

## 2.2 Semiconductor as Photo-anode

In general, dye-sensitized solar cells (DSSCs) comprise several key components, including a photo-anode, sensitized dyes, redox electrolytes, and a counter electrode. The photoanode plays a crucial role as one of the central components in DSSCs, thus significant research efforts have been dedicated to its development. Semiconductor materials, such as $TiO_2$, ZnO, SnO2, Nb2O5, and ZrO2, have been widely investigated and reported as potential photoanode materials. Among these semiconductor materials, $TiO_2$ has shown great promise and garnered significant attention due to its favorable characteristics for practical applications in DSSCs [40].

Taehan Chŏn'gi Hakhoe et al. [41] discussed the photoanode of DSSCs, which typically comprises a semiconductor metal oxide, which serves as a substrate for dye adsorption. Typically employed in paste form, this material plays a critical role in determining the power conversion efficiency of DSSCs. The PCE is highly influenced by various factors, including morphological characteristics, surface area, porosity, crystallinity, and the conduction band properties of the semiconductor materials. Notably, a higher surface area of the material facilitates enhanced dye absorption, thereby contributing to improved performance.

Ming-Jer Jeng et al. [42] revealed that the optimal thickness of $TiO_2$ layers in dye-sensitized solar cells depends on the particle sizes of the $TiO_2$ layers to achieve maximum efficiency. Comparative studies demonstrated that DSSCs prepared with triple $TiO_2$ layers, each with different particle sizes, exhibit higher solar efficiency than those with double $TiO_2$ layers of the same thickness. Moreover, the experimental findings indicate that larger particle sizes of $TiO_2$ in the top layer and smaller particle sizes in the bottom layer of double-layer structures can result in higher solar efficiency. This outcome is attributed to stronger back-scattering of light and increased surface area, respectively. Similarly, for triple-layer structures, DSSCs with larger particle sizes in the top layer and smaller particle sizes in the bottom layer exhibit enhanced solar efficiency. However, the optimal particle sizes in the middle layer are contingent upon the sizes in the bottom and top layers. Hence, to enhance solar efficiency, it is advisable to carefully select a synergistic blend of particle sizes for the middle layer.

Wei Wang et al. [43] demonstrated the significant impact of the light-scattering effect on the light-harvesting capability of $TiO_2$ photoanodes, surpassing the importance of dye adsorption capacity, even when the thickness remained constant. Specifically, the light-scattering effect exhibited a remarkable enhancement in light absorption within the red region of the solar spectrum. Remarkably, the cell incorporating an optimized high dye adsorption layer and a high light-scattering three-layer configuration achieved the highest power conversion efficiency of 7.52%. This efficiency surpassed that of the cell lacking the light-scattering layer by 9.5%, which attained an efficiency of 6.87%. To investigate the light-scattering effect, three types of $TiO_2$ layers, including the light-scattering layer, were individually fabricated and in a layer-by-layer fashion. The investigation involved analyzing the diffused reflectance spectra of the $TiO_2$ layers and the incident photon-to-current efficiency (IPCE) of the corresponding DSSCs. Additionally, the photovoltaic properties of DSSCs were examined through photoelectric measurements, comparing the cells with and without the LSL and varying thicknesses of the $TiO_2$ layer.

Zhong-Sheng Wang et al. [44] demonstrated a simple method to enhance dye adsorption and improve the performance of DSSCs. This was achieved by growing a thin electronic insulating coating of CaCO3 on the surface of $TiO_2$, resulting in significant improvements in both photocurrent density and open-circuit voltage. By controlling the amount of CaCO3 coating to as little as 1 wt%, notable enhancements in Jsc and Voc were observed, leading

to a significant overall improvement in power conversion efficiency. However, when a larger amount of coating was applied, the increased insulating effect hindered electron injection and reduced Jsc, even though Voc was further enhanced. This highlighted the importance of finding an optimal balance between electron recombination suppression and efficient electron injection to maximize power conversion efficiency. One promising solution involves the formation of a core-shell composite structure by coating the $TiO_2$ surface with semiconductor materials, thereby offering a potential strategy to mitigate charge recombination and enhance overall device performance.

SArunmetha et al. [45] developed the synthesis process for the sulfur-doped $TiO_2$. By employing a simple chemical method during the extraction of $TiO_2$ precursor from rutile sand, sulfur was successfully doped into the material. They revealed that $S/TiO_2$ exhibited several advantageous properties, including a smaller crystallite size of 10 nm, a higher surface area of 86 $m^2/g$, and a spherical morphology of individual grains. Importantly, the introduction of sulfur in $S/TiO_2$ resulted in improved UV-Visible absorption, leading to enhanced generation of photogenerated electrons and holes, as well as reduced charge carrier recombination during photocatalytic reactions. In comparison to pure $TiO_2$ cells, the efficiency of $S/TiO_2$ cells was observed to be twice as high. The overall power conversion efficiency (PCE) of $S/TiO_2$ cells showed a significant improvement, reaching 4.32%, while the external quantum efficiency (EQE) for $S/TiO_2$ cells rose to 32%. These findings highlight the potential of $S/TiO_2$ as a highly efficient material for achieving high-performance dye-sensitized solar cells.

Anupam Agrawal et al. [46] investigated the performance and characteristics of dye-sensitized solar cells prepared using two different deposition techniques: screen printing (SP) and doctor blade (DB). Researchers explained the preparation of $TiO_2$ paste from $TiO_2$ nanoparticle powder and organic binders suitable for both SP and DB techniques. Various characterizations were conducted, revealing that the SP-deposited $TiO_2$ layers exhibited lower crack widths and better dye loading compared to the DB-deposited layers. The I-V measurements demonstrated higher performance in SP-based DSSCs compared to DB-based DSSCs. Specifically, the PCE improved from 6.72% to 7.25% for Screen Printing-based DSSCs and from 4.86% to 6.13% for Doctor Blade-based DSSCs, the result includes evaluated various parameters like series resistance, saturation current, and ideality

factor. Additionally, the transparency and color effects of the DSSCs were analyzed using average visible transmittance, color rendering index, and correlated color temperature. Alagesan Subramanian et al. [47] introduced that the improved performance of the multilayer-structured electrode was attributed to several factors. Firstly, it displayed a higher dye loading capacity, allowing for greater absorption of light. Additionally, the multilayer structure facilitated efficient light harvesting throughout the electrode. Lastly, the charge transportation from the top layer to the bottom layer was improved by the presence of $TiO_2$ nanotubes, contributing to enhanced overall charge transfer and reduced recombination. They discussed an advantage of the hierarchical multilayer system is that it eliminates the need for specialized techniques to increase film thickness while maintaining high quality for improved dye adsorption. This provides a practical and effective approach for enhancing the performance of DSSCs without the requirement of additional complex fabrication processes.

Tharmakularasa Rajaramanan et al. [48] synthesized N-doped TiO2 nanoparticles by varying the volumetric ratio of P25-$TiO_2$ and ammonium hydroxide (NH4OH) through a solid-state reaction. These nanoparticles were then used to prepare films, which were sintered at 500°C. The facile solid-state reaction successfully synthesized N-doped $TiO_2$ nanoparticles with systematically varied amounts of NH4OH, which were effectively integrated into the fabrication of dye-sensitized solar cells (DSSCs). The X-ray diffraction analysis revealed that the introduction of N doping had no discernible effect on the crystal structures of $TiO_2$, thereby confirming the structural integrity of $TiO_2$ remained unaffected by the N doping process. Nitrogen presence was confirmed through X-ray photoelectron spectroscopy and energy-dispersive X-ray analysis. Scanning electron microscopy and transmission electron microscopy images showed agglomeration of nanoparticles at higher N doping levels. BET, BJH, and UV-visible spectroscopy results indicated that optimal N doping increased the pore diameter of $TiO_2$ particles, leading to higher dye adsorption. J-V measurements revealed that the DSSC assembled with a 20N-$TiO_2$ photoanode exhibited a 20% higher power conversion efficiency (PCE) of 6.16% compared to the control device with a PCE of 5.15%. This improvement in PCE was mainly attributed to enhanced current density (JSC) resulting from increased visible light absorption and reduced charge recombination. Among reported studies on DSSCs using N-doped P25-$TiO_2$ photoanodes, our method achieved the highest PCEs.

## 2.3 Dyes in DSSCs

### 2.3.1 Organometallic dyes

Praveen Naik et al. [49] developed a co-sensitized dye-sensitized solar cell by incorporating four simple aniline-based dyes (A1-4) with different acceptor/anchoring moieties into an N3 dye. The co-sensitizer A2, which carried N, N-dimethyl barbituric acid as the anchoring/accepting moiety, exhibited superior photovoltaic performance compared to N3 alone at various concentrations. The most efficient device was fabricated using 0.3 mM co-sensitizer A2 and 0.2 mM N3 sensitizer, achieving a power conversion efficiency of 7.02%. This device displayed a photocurrent density of 15.27 mA·cm−2, a voltage at open circuit ($V_{OC}$) of 0.671 V, and a fill factor of 0.6847. Electrochemical impedance spectroscopy (EIS) studies indicated that the co-sensitized devices effectively suppressed undesired charge recombination, leading to improved $V_{OC}$. These findings underscore the importance of selecting suitable co-sensitizers and their concentrations to enhance the performance of DSSCs sensitized with Ru-II complexes. The research highlights a promising approach to optimize DSSC efficiency using co-sensitization strategies.

Subramaniam Kamalesu et al. [50] reported the successful synthesis and characterization of a novel monometallic-Ruthenium(II)complex(RNPDA) containing a 4-Nitro-phenylenediamine ligand (NPD-PC) with dual anchoring units. The RNPDA complex exhibited favorable photophysical and redox properties, along with excellent thermal and photostability. The design of NPD-PC enabled the binding of RNPDA to the $TiO_2$ surface through the simultaneous use of two anchoring groups, thereby enhancing the efficiency of the fabricated dye-sensitized solar cell (DSSC). The incorporation of dual anchoring groups improved the spectral response, reduced recombination resistance, prolonged electron lifetime, and increased overall efficiency. The DSSC constructed using the RNPDA sensitizer achieved a power conversion efficiency (PCE) of 3.42%, with a Voc of 0.79 V and a JSC of 7.12 mA/cm$^2$.

Jiayan Cong et al. [51] introduced an organic JY1 dye functionalized with an electron-withdrawing nitro group that was synthesized and investigated. Surprisingly, higher efficiencies in dye-sensitized solar cells (DSSCs) were achieved by applying a reverse

voltage. The results revealed that the nitro group attached to the $TiO_2$ surface caused a decrease in dye absorption but enhanced the dye's ability to inject electrons into the $TiO_2$ conduction band. As a result, the DSSCs exhibited increased efficiency with JY1. Interestingly, during the measurement of the photoelectric properties of DSSCs fabricated with JY1 under simulated AM 1.5G illumination (100 mW $cm^{-2}$), a notable phenomenon was observed. Initially, the efficiencies were relatively low (approximately 0.15%). However, after a period of device testing, the efficiencies of the DSCs increased approximately five-fold to 0.81% (Jsc = 2.12 $mA.cm^{-2}$, Voc = 0.59 V, ff = 0.66).

Yan Hao et al. [52] designed a novel blue-color D-π-A organic sensitizer (DB) and synthesized it for dye-sensitized solar cells (DSSCs) utilizing cobalt-based redox systems. The DB dye achieved an energy conversion efficiency of 7.3% under one sun AM 1.5G conditions. To further enhance the performance, a co-sensitization strategy was employed by incorporating an additional D35 dye. The co-sensitized device exhibited a remarkable power conversion efficiency of 8.7%, with increased current density due to complementary absorption from the two dyes. This performance surpassed that of individual devices sensitized solely by DB (7.3%) or D35 (5.5%) under the same fabrication conditions. The presence of D35 reduced recombination at the $TiO_2$/dye and electrolyte interface, as well as between electrons in $TiO_2$ and oxidized dyes. The study demonstrated the feasibility of utilizing two distinct organic dyes with different absorption spectra in combination with cobalt complex-based redox systems. This co-sensitization approach effectively utilized a wider range of light in the solar spectrum while enhancing surface coverage on $TiO_2$.

## 2.3.2 Metal-free dye

Govind Sharma et al. [53] provided an overview of recent advancements in metal-free organic sensitizers and their photovoltaic characteristics in DSSCs. While ruthenium-based dyes have demonstrated high power conversion efficiencies and stability, their commercial use is limited by their high cost and environmental impact. In contrast, metal-free organic sensitizers offer a sustainable solution with their low-cost and environmentally friendly nature. This review paper highlights the latest research on metal-free organic dyes as sensitizers for DSSCs. However, challenges such as low efficiency and stability still need

to be addressed. Ongoing efforts include structural modifications of these dyes by optimizing suitable donor-acceptor groups and π-spacers for improved device performance.

Liu Yang et al. [54] presented the design and synthesis of a series of novel metal-free organic sensitizers based on N-annulated perylene derivatives. These sensitizers incorporate triphenylamine derivatives as additional electron donors and steric structures, varying numbers of thiophenes as conjugated linkers, and 2-cyanoacetic acid as an electron acceptor. The introduction of methoxy groups to the triphenylamine moiety effectively reduces charge recombination. Furthermore, the direct attachment of the NP unit to the cyanoacetic acid acceptor unit, without a thiophene π-spacer, enhances electron injection into the $TiO_2$ film. The resulting DSSCs utilizing these organic dyes exhibit remarkable overall conversion efficiencies ranging from 4.90% to 8.28%. Notably, the solar cells based on NPS-4 demonstrate the best performance, with an efficiency (η) of 8.28%, photocurrent density (Jsc) of 16.50 mA cm-2, the voltage at open circuit (Voc) of 0.734 V, and fill factor (ff) of 0.684. Ongoing research in the laboratory aims to further improve the photovoltaic performance of these dyes.

Praveen Naik et al. [55] reported the molecular design, synthesis, and characterization of three new metal-free organic dyes, D1-3, with a D-D-π-A configuration for their application as sensitizers and co-sensitizers in dye-sensitized solar cells. These dyes feature a carbazole donor scaffold, a 4-methoxyphenyl auxiliary donor, and different acceptor/anchoring groups, including cyanoacetic acid, 2,4-thiazolidinedione, and barbituric acid. Extensive photophysical, electrochemical, and theoretical studies were conducted to evaluate their potential as active sensitizers. The DSSCs fabricated using these dyes showed promising results. Among the dyes, D1 exhibited the highest power conversion efficiency (PCE) of 2.20%. When D3 was used as a co-sensitizer with NCSU-10 dye, the DSSC achieved an improved PCE of 8.32%, while NCSU-10 alone showed a PCE of 8.25%. The co-sensitization strategy effectively suppressed charge recombination, resulting in longer electron lifetimes. This research highlights the potential for further enhancing DSSC performance through suitable molecular matching between main sensitizers and co-sensitizers.

K. Narayanaswamy et al. [56] synthesized two metal-free organic dyes KNS1 and KNS2 based on the triphenylamine (TPA) core structure. These dyes incorporated triphenylamine

and thiophene moieties as electron donors, and cyanoacrylic acid and rhodanine-3-acetic acid units as electron acceptors. Dye-sensitized solar cells using nanocrystalline TiO2 were fabricated to investigate the impact of different anchoring groups on their photovoltaic performance. The DSSCs employing KNS1 and KNS2 achieved power conversion efficiencies of approximately 2.01% and 2.95%, respectively. Notably, the addition of chenodeoxycholic acid (CDCA) to the dye solution resulted in significant enhancements in PCE, reaching 3.53% and 3.00% for KNS1 and KNS2, respectively. KNS2 demonstrated superior electron injection efficiency and reduced recombination rates, leading to higher $J_{sc}$, $V_{oc}$, and PCE values compared to KNS1. Additionally, the coadsorption of CDCA improved the $J_{sc}$ and $V_{oc}$ for KNS1, highlighting the potential of these dyes as small molecular co-sensitizers. Although the photo conversion efficiency of these dyes may be limited due to their narrow optical absorption window and lower $V_{oc}$, the synthetic strategy employed here holds promise for designing new molecules to enhancing DSSC photovoltaic performances.

Haijing Feng et al. [57] Constructed, synthesized, and designed two novel coumarins in the category of metal-free sensitizers based on a D-π-A-π-A to enhance the intramolecular charge transfer (ICT) process and minimize energy loss, an additional p-bridge was introduced between the coumarin and benzothiadiazole segments, reducing the dihedral angle between them. Compared with NKX-2677, which is the most efficient in the category of coumarin sensitizer. CS-1 exhibited the best light-harvesting capability and the narrowest band gap between the HOMO and LUMO levels, thanks to its excellent planarity. However, the overly narrowed band gap of CS-1 resulted in inefficient charge injection from the LUMO to the conduction band of $TiO_2$, leading to poor photovoltaic performance. On the other hand, CS-2, with a slightly more negative LUMO level, showed improved charge injection efficiency despite a slightly weakened light-harvesting capability. DSSCs sensitized with CS-2 achieved a remarkable record PCE of 8.03%, along with high stability after a 1000-hour aging test. These findings emphasize the significance of optimal planarity for enhancing energy levels and photovoltaic performance in organic sensitizers, providing valuable insights for future development.

## 2.3.3 Natural Dye

Ahmed M. Ammar et al. [58] extracted from red cabbage, onion peels, and spinach were employed as sensitizers for DSSCs. Optical and structural properties of the dyes and fabricated cells were examined, compared with N719 ruthenium complex dye. The degradation in the PCE of N719 and natural-based DSSCs was monitored. DSSCs utilizing natural sensitizers and N719 were prepared, and their photoelectrochemical parameters were analyzed. The DSSCs with spinach extract exhibited the following values over a week: Jsc ($mA \cdot cm^{-2}$) ranging from 0.41 to 0.26, Jm (mA·cm-2) ranging from 0.309 to 0.181, Voc (V) ranging from 0.59 to 0.55, Vm (V) ranging from 0.46 to 0.38, FF (%) ranging from 58.76 to 48.10, and η (%) ranging from 0.17 to 0.082. DSSCs with a photoelectrode thin film of 10% $TiO_2$ achieved the highest photoelectric conversion efficiency of 2.239%. The DSSC based on chlorophyll dye demonstrated the highest performance among the naturally extracted dyes, with a power conversion efficiency of 0.17%.

Monzir S. Abdel-Latif et al. [59] focused on the investigation of natural dyes extracted from three different trees as photosensitizers for dye-sensitized solar cells (DSSCs). A total of eleven natural dyes were extracted from various parts of olive, Lycium shawii, and zizyphus trees, including flowers, fruits, leaves, bark, and roots. The absorption spectra of these dyes were analyzed within the spectral range of 400 nm to 750 nm. Furthermore, the J-V characteristic curves of all the fabricated cells were measured, plotted, and carefully examined. Parameters related to the performance of the solar cells were determined to assess their efficiency. Additionally, impedance spectroscopy was performed on the cell that exhibited the best performance. The results indicated that the DSSCs sensitized with plant leaves, particularly due to the presence of chlorophyll a, showed higher efficiency compared to those sensitized with other parts of the trees. The DSSC sensitized with zizyphus leaves demonstrated the highest conversion efficiency of 0.40%, while the DSSCs sensitized with roots and barks exhibited the lowest response.

Fahmid Kabir et al. [60] focused on the utilization of natural anthocyanin dye extracted from red spinach (*Amaranthus dubius)* as a sensitizer to enhance the performance of dye-sensitized solar cells (DSSCs). The crude red spinach dye extract was subjected to a solvent

extraction process to remove unwanted impurities, resulting in a refined anthocyanin dye extract. The cell parameters of the DSSCs sensitized with the crude extract showed short circuit current (Isc) of 0.642 mA, open-circuit voltage (Voc) of 0.329 V, fill factor (FF) of 0.434, and efficiency of 0.091%. On the other hand, the DSSCs sensitized with the refined anthocyanin dye extract exhibited improved photo-electrical properties, with Isc ranging from 0.642 mA to 1.385 mA, Voc ranging from 0.329 V to 0.379 V, and FF ranging from 0.434 to 0.469. The DSSC sensitized with the purified anthocyanin dye demonstrated an efficiency of 0.247%, which was approximately 2.7 times higher than that of the DSSC sensitized with the crude red spinach extract. Additionally, the cell stability of the refined dye-based DSSC was comparatively better than that of the crude dye-based DSSC after a 48-hour aging period. This research showcased the potential of refining natural dye sensitizers to enhance the performance and stability of DSSCs, paving the way for further exploration in this field.

I Nyoman Setiawan et al. [61] extracted natural dyes using the maceration method, which involved soaking fine powder from red dragon fruit peel in distilled water mixed with 10% citric acid. Three different weight ratios of material to solvent (1:4, 1:6, and 1:8) were used for the extraction process, which lasted for 24 hours. The FTIR analysis confirmed the presence of a hydroxyl group in the samples, which is an essential component of the anthocyanin structure. This hydroxyl group serves as an adhesive between pigment compounds and a thin layer of $TiO_2$ on FTO. The fabricated dye-sensitized solar cells (DSSCs) were evaluated under 500 $W/m^2$ lighting conditions. The results showed that while the generated voltage was satisfactory, the obtained current was relatively low due to high resistance in the $TiO_2$ semiconductor electrode layer and the fast drying of the electrolyte. Although these efficiencies are still relatively low, they provide encouraging results and suggest the potential for further research focused on discovering new naturally sensitive substances. UV-Vis characterization demonstrated absorption in the visible area, with varying absorbance power, photon energy, and absorption coefficient (α) among the three dye solution samples. The DSSCs utilizing the 1:8 ratio showed the best performance, with Voc = 0.47 V, Jsc = 23.46 $\mu Acm^{-2,}$ Fill Factor = 0.480, and an efficiency of 0.029%.

## 2.3.4 Synthetic Dye

Taher M. El-Agez et al. [62] fabricated dye-sensitized solar cells by utilizing TiO2 nanoparticles as the semiconducting layer. Eight synthetic dyes, namely eosin Y, aniline blue, bromophenol blue, alcian blue, methyl orange, crystal violet, fast green, and carbol fuchsine, were employed as photosensitizers for the nano-crystalline $TiO_2$ photo-electrodes. The characterization of these dyes was conducted using UV-VIS spectrophotometry. The photovoltaic properties of the DSSCs were thoroughly investigated. Under the illumination of 100 $mW/cm^2$, the photovoltaic parameters of the fabricated DSSCs were determined. The DSSC sensitized by eosin Y exhibited the best performance among the tested dyes, achieving an impressive cell efficiency of 0.399%. This outcome highlights the potential of eosin Y as a highly efficient sensitizer for enhancing the performance of DSSCs. The findings contribute to the advancement of synthetic dye-based sensitization in the development of efficient and sustainable solar energy conversion systems.

Nurhidayani et al. [63] studied the utilization of Asphalt Buton (Asbuton) extract and methylene blue as photosensitizer dyes in Dye-Sensitized Solar Cells. The research aims to investigate the performance of Asbuton extract and MB as dyes in generating voltage-current responses under visible light irradiation. The $TiO_2$/Ti NTAs electrode was successfully synthesized using an anodizing method, and XRD analysis confirmed the formation of anatase crystals. Furthermore, the morphology analysis revealed the formation of nanotubes coated with Asbuton extract. The DSSC system was constructed using a sandwich structure and evaluated using a Multimeter Digital with a Potentiostat instrument. The current and potential characteristics over time indicated that the Asbuton extract exhibited high-performance results, with 14,000µV and 0.844µA after 30 seconds, while the MB dyes showed values of 8,000µV and 0.573µA, respectively. These findings highlight the potential of Asbuton extract, sourced from Buton Island in Southeast Sulawesi, Indonesia, as a natural dye for the DSSC system.

Bandana Ranamagar et al. [64] investigated the properties of Rhd and its metal complexes, the study synthesized Rhd using a microwave-assisted condensation method involving rhodamine hydrazide and 2-Amino-3-formylchromone. Ultraviolet-visible and

fluorescence spectroscopy were employed for characterization purposes. Furthermore, DSSCs were fabricated using Rhd and its metal complexes, specifically with aluminum (Al3+) and chromium (Cr3+) ions. The solar cell sensitized with Rhd and Cr3+ demonstrated the highest solar-to-electric power efficiency of 0.16%. These findings contribute to the understanding of the potential application of Rhd as a turn-on, fluorescent sensor for Al3+ and Cr3+ ions, emphasizing its advantages over other metal ions. The study also highlights the significance of charge transfer resistance and electron lifetime in enhancing the efficiency of DSSCs.

### 2.3.5 Natural Dye with Synthetic Dye

G. Richhariya et al. [65] composed a synthetic organic dye and a natural dye, which had been explored as a promising approach to enhance the overall performance of dye-sensitized solar cells (DSSCs). Specifically, a combination of Rhodamine dye (synthetic organic) and Hibiscus sabdariffa extract (natural dye) was utilized as the sensitizer for DSSC fabrication. UV-Vis absorption analysis revealed a high molar extinction coefficient and significant spectral overlap in the maximum absorption region. Notably, the co-sensitized dye exhibited broader absorption in the range of 440-560 nm. The photovoltaic results demonstrated the highest short circuit current of 4.02 $mAcm^{-2}$ and the highest incident power conversion efficiency of 1.23%. These improvements can be attributed to efficient panchromatic light harvesting and favorable optical activity. Furthermore, the adsorption of the co-sensitized dye on the $TiO_2$ surface was enhanced, owing to the smaller size of the semiconductor surface-aggregated pigment molecules. Electrochemical analysis indicated reduced charge transfer resistance in the co-sensitized dye, contributing to the superior performance of the DSSCs. The experimental findings highlight the prominence of co-sensitized dyes for enhancing the performance of dye solar cells.

Roohollah Nakhaei et al.[66] presented a new simple and low-cost approach to sensitization of DSSCs. Four natural dyes were utilized as co-sensitizers in conjunction with the N719 synthetic dye, creating a wide photoabsorption spectrum. The results indicated that the conventional cocktail method, which mixes all dyes, did not show significant improvement compared to using a single dye. This limitation was attributed to the limited adsorption of

natural dyes in the presence of the strongly binding synthetic dye on the $TiO_2$ nanoparticles. The sequential method, which applies dyes sequentially, also suffered from limited dye adsorption due to a scarcity of available $TiO_2$ anchoring sites. XRD and FESEM analyses confirmed that the layer created with an acid concentration of 0.25M using the low-temperature process exhibited good quality in terms of morphology, crystallinity, and porosity. The proposed method achieved the highest efficiency of 3.48%, outperforming the cocktail and sequential methods, which achieved efficiencies of 1.88% and 2.29%, respectively. The results of the study demonstrated that the proposed approach improved charge injection and transportation by enabling separated dye adsorption. This resulted in improved dye loading and spectral expansion, leading to an efficiency of 3.48% highlighting the superior performance of the proposed method compared to the cocktail and sequential methods.

G. Richhariya et al. [67] fabricated using a mixed dye derived from *hibiscus sabdariffa* and eosin Y. A nanostructured mesoporous film was created from titanium dioxide ($TiO_2$) to serve as the electrode. The energy conversion efficiencies of hibiscus dye, eosin Y dye, and the mixed dye were measured as 0.41%, 1.53%, and 2.02% respectively. The performance of the mixed dye DSSC surpassed that of the individual hibiscus and eosin Y dyes, thanks to the inclusion of a synthetic organic dye. This enhancement was attributed to improved light absorption, particularly in the higher energy range ($\lambda$ = 440-560 nm), as observed in the absorption spectra of the dyes on the $TiO_2$ electrode. The mixed dye exhibited a short circuit current density (Jsc) of 4.01 mA/cm2, an open circuit voltage (Voc) of 0.67 V, a fill factor (FF) of 0.60, and an energy conversion efficiency ($\eta$) of 2.02%. However, the photovoltaic performance of the cell using mixed dye was inferior to that of commercial synthetic dyes.

## 2.3.6 Development of DSSCs

Jung-Min Ji et al. [68] introduced a series of new organic chromophores based on 4-hexyl-4H-thieno[3,2-b]indole (HxTI) that have been developed through structural engineering of the electron donor (D) group in the D–HxTI–benzothiadiazole-phenyl-acceptor platform. Different fluorenyl moieties, including unsubstituted fluorenyl (SGT-146) and hexyloxy (SGT-147), decyloxy (SGT-148), and hexyloxy-phenyl substituted (SGT-149) fluorenyl

moieties, were used. The results show that the bulkiness of the donor groups improves the photovoltaic performance of dye-sensitized solar cells (DSSCs). Particularly, DSSCs based on SGT-149 demonstrate high power conversion efficiencies (PCEs) of 11.7% and 10.0% with a [Co(bpy)3]2+/3+ (bpy = 2,2′-bipyridine) and an I−/I3− redox electrolyte, respectively. Additionally, co-sensitization of SGT-149 with an SGT-021 porphyrin dye using a simple "cocktail" method yields state-of-the-art PCEs of 14.2% and 11.6% with a [Co(bpy)3]2+/3+ and an I−/I3− redox electrolyte, respectively.

H.P. Wante et al. [69] utilized the atmospheric dielectric barrier discharge (DBD) technique as a surface modification method for polymer substrates. Through contact angle analysis, it is evident that the treated substrate exhibits a significant reduction of approximately 60% in contact angle compared to the untreated substrate. When this treated substrate is employed in dye-sensitized solar cells (DSSCs), it shows an improved power conversion efficiency of 2.25% compared to DSSCs based on untreated substrates, which yield a lower PCE of 0.94%. The enhancement in PCE observed in the DSSCs using the treated substrate is attributed to the improved bonding between the substrate and the transparent semiconducting material (TiO2). This suggests that the DBD modification of polymers has the potential to enhance the efficiency of DSSCs by improving the adhesion of the particles to the substrate, surpassing the conventional cleaning method.

A. Azmar, et al. [70] prepared gel polymer with the help of Blends of poly(methyl acrylate) (PMA) and poly(vinyl acetate), incorporating tetrapropylammonium iodide(TPAI) salt, 1-butyl-3-methylimidazolium iodide (BMII) ionic liquid, and ethylene carbonate (EC) plasticizer. The concentration of EC, represented by WEC, was varied to investigate its impact on the performance of dye-sensitized solar cells. The addition of EC to PMA/PVAc-TPAI-BMII improved the efficiency of the DSSCs by enhancing the short circuit current density (Jsc) through increased conductivity. A comparison between DSSCs with TPAI-BMII-EC liquid electrolyte and PMA/PVAc-TPAI-BMII-EC gel electrolyte revealed that although PMA/PVAc reduced Jsc and efficiency (η), it enhanced the stability of the DSSCs by suppressing recombination losses. The interaction between the components in PMA/PVAc-TPAI-BMII-EC was confirmed by FTIR and DSC studies. EC increased the conductivity by facilitating ion dissociation and enhancing polymer chain flexibility. The highest efficiency of 9.67% was achieved with a gel-like electrolyte containing WEC = 0.20. Despite lower efficiency, DSSCs with PMA/PVAc demonstrated better stability

retention after 288 hours compared to DSSCs without PMA/PVAc. The authors declare no competing interests.

D.A. Chalkias et al. [71] prepared a blended polymer as a cost-effective and straightforward method for preparing advanced polymer electrolytes in dye-sensitized solar cells. Extensive investigation of PVP/PEG blend-based polymer electrolytes has revealed intriguing characteristics. This study pioneered the use of a polymer electrolyte exhibiting "polymer-in-salt" conduction properties, resulting in high conductivity and reduced electron-hole recombination rates within the solar cells. The application of PVP/PEG blend-based polymer electrolytes in DSSCs demonstrated a remarkable 30% improvement in efficiency compared to conventional PVP-based and PEG-based electrolytes. Additionally, the incorporation of two commonly used chemical additives found in liquid-state electrolytes of DSSCs was explored in the optimal polymer blend electrolyte, shedding light on their mechanisms in quasi-solid-state DSSCs. The highest achieved energy conversion efficiency of 8.21% by the DSSCs employing the best-performing PVP/PEG blend-based polymer electrolyte ranks among the highest reported for non-composite iodide-based polymer electrolytes. These findings present a promising alternative to commercially available liquid-state electrolytes, with the potential for further optimization in the composition of PVP/PEG blend-based polymer electrolytes.

Dafu Wang et al. [72] represented third-generation solar cells, which offer advantages such as ease of fabrication and relatively high power conversion efficiency. However, the commonly used dyes in DSSCs are both expensive and toxic, limiting their practicality. In this study, they explored the potential of non-toxic food dyes, namely Amaranth, Sunset Yellow, and Erythrosin B, for DSSC applications. Notably, for the first time, they combined two food dyes in DSSCs, resulting in a significant increase in PCE. Moreover, established a correlation between the PCE and the composition of the combined dyes. Among the tested configurations, the ZnO-based DSSC incorporating a blend of Amaranth and Erythrosin B dyes demonstrated the highest PCE of 2.64%. These findings present a promising avenue for utilizing non-toxic food dyes in DSSC technology, contributing to the development of environmentally friendly and cost-effective solar energy conversion systems.

Ismail Althagaf et al. [73] engineered five organic compounds (IS1-5)as DSSC sensitizers, and their performance was further improved through co-sensitization. Co-sensitizing IS1-5 with N-719, a ruthenium-based dye, resulted in higher VOC values compared to individual N-719. IS-5 showed the greatest impact on N-719's photovoltaic efficiency, achieving a PCE of 8.09%, JSC of 19.23 mA.cm^-2, and VOC of 0.680V, surpassing N-719's PCE of 7.61%, JSC of 18.59 mA.cm^-2, and VOC of 0.658V. IS-4 and IS-5, containing ANO2 and ACOOH anchoring species, respectively, exhibited broadening in their spectra and a red-shift in their lowest energy band due to extended conjugation. IS-4 and IS-5 exhibit the highest molar extinction coefficients and display a bathochromic shift to the intramolecular charge transfer band, as observed from their UV/Vis spectra.

## 2.4 Gap of Knowledge

Despite their promising potential, DSSCs have not yet achieved widespread commercialization. One of the primary knowledge gaps lies in developing scalable and cost-effective manufacturing processes for DSSCs. Scaling up the production of DSSCs while maintaining high efficiency and reliability poses significant challenges that require further research and development. The long-term performance of DSSCs is a critical concern for their practical application. Knowledge gaps exist in understanding the degradation mechanisms and stability issues that affect DSSCs over extended periods of operation. Factors such as dye degradation, electrolyte evaporation, and electrode corrosion can contribute to a decrease in efficiency over time. Further research is needed to identify and address these issues to ensure the long-term stability and durability of DSSCs. DSSCs are known to be sensitive to environmental conditions, such as temperature, humidity, and UV exposure. Stability issues arise due to the vulnerability of the electrolyte and the potential for dye degradation. Enhancing the stability of DSSCs is a significant challenge that requires a deeper understanding of the degradation mechanisms and the development of more robust materials and designs.

One potential knowledge gap that exists pertains to the limited comprehension surrounding the testing of dye-sensitized solar cells (DSSCs) under natural environmental conditions. Although most researchers adhere to the standard testing conditions (STC), the understanding of how DSSCs perform in actual natural environments remains lacking. Additionally, another gap lies in the fabrication process of DSSCs. While conventional

fabrication processes for DSSCs are well-documented, there is a notable absence of a comprehensive, simplified process encompassing all stages, ranging from cleaning to fabrication. Furthermore, limited research is available on the comparative analysis of synthetic dye, acrylic dye, and agro-waste-based dye as potential sensitizers for DSSCs. These alternative sources hold promise for the fabrication of DSSCs. Given the potential benefits of utilizing natural dyes, including sustainability and cost-effectiveness, it is imperative to investigate the performance and stability of DSSCs employing agro-waste-based dyes. Additionally, the performance of DSSCs employing acrylic dyes is also constrained, thus warranting a thorough examination of their performance under natural environmental conditions.

## 2.5 Probable Solutions

To address the knowledge gaps mentioned, several potential solutions can be pursued. Firstly, to improve the understanding of DSSCs under natural environmental conditions, further research should be conducted specifically focusing on testing methodologies and performance evaluation in realistic outdoor settings. This would involve designing experiments that replicate natural environmental factors such as varying light intensities and exposure to different weather conditions. By systematically investigating the behavior of DSSCs under these conditions, a more comprehensive understanding can be obtained. Secondly, to bridge the gap in the fabrication process of DSSCs, efforts should be directed toward developing a simplified and standardized procedure that encompasses all stages, including cleaning, dye loading, and fabrication. This could involve conducting systematic studies to identify the most effective cleaning methods and optimizing the fabrication parameters to ensure reproducibility and efficiency. The development of a standardized fabrication process would contribute to greater consistency and reliability in DSSCs production.

To compare the performance of synthetic organic dye, acrylic dye, and agro-waste-based dye as sensitizers for DSSCs, a comprehensive comparative analysis should be undertaken. This would involve evaluating the absorption range, efficiency, and stability of DSSCs utilizing these different dye sources. A comprehensive understanding of the underlying mechanisms and performance characteristics of each dye type should be explored to gain

insights into their potential applications in DSSCs. Furthermore, to assess the performance and stability of DSSCs employing agro-waste-based dyes, extensive research should be conducted. This would involve studying the effect of different agro-waste sources, extraction methods, and dye sensitization processes on the performance of DSSCs.

Lastly, to overcome the limitations associated with acrylic dye-based DSSCs, a thorough examination of their performance under natural environmental conditions is crucial. This can be achieved by conducting field studies and monitoring the performance of DSSCs employing acrylic dyes over an extended period. By assessing the influence of natural environmental factors on the performance and stability of acrylic dye-based DSSCs, insights can be gained to optimize their design and fabrication processes.

Overall, these proposed solutions aim to address the existing knowledge gaps in the testing and fabrication of DSSCs and provide a comprehensive understanding of different dye sensitizers. By pursuing these research avenues, advancements can be made toward improving the efficiency, stability, and practical viability of DSSCs in real-world applications.

## 2.6 Scope of the Work

This thesis presents a comprehensive and formalized description of the systematic process involved in the fabrication of dye-sensitized solar cells (DSSCs). This work aims to provide a clear and concise framework for researchers and practitioners in the field, facilitating the replication and understanding of the DSSC fabrication procedure. The described process encompasses the key stages, materials, and equipment involved in the successful assembly of DSSCs, thereby enabling the efficient utilization of this renewable energy technology.

1. Design of Dye Sensitized Solar Cells (DSSCs): The project will involve exploring and developing different designs for DSSCs using alternative dyes. This includes researching various dye materials, such as organic and inorganic dyes, and their potential for enhancing the performance of DSSCs.

2. Fabrication Techniques: The project will investigate different fabrication techniques for constructing DSSCs with alternative dyes. This includes experimenting with electrode materials, electrolytes, and other components to optimize the overall efficiency and stability of the solar cells.

3. Comparative Performance Analysis: A significant aspect of the project involves conducting a comparative analysis of the performance of alternative dye-based solar cells. This analysis will assess factors such as power conversion efficiency under natural environment conditions.

4. Evaluation of Light Absorption The project will focus on studying the light absorption properties of alternative dyes. This evaluation will help identify dyes that can effectively capture and convert solar energy.

5. Selection of Materials: Upon comprehensive analysis of existing research in the field, it becomes evident that the selection of an appropriate photoanode and counter electrode for Dye-Sensitized Solar Cells (DSSCs) is crucial. Additionally, the choice of a suitable dye with an optimal solar spectrum absorption rate is essential as it directly influences the overall power efficiency of the DSSCs. Therefore, careful consideration and selection of these components are imperative for the successful design and performance of DSSCs.

The first chapter of the thesis provides an overview of the energy scenarios and establishes the objectives and justification for researching Dye Sensitized Solar Cells. It highlights the current energy challenges and the need for sustainable and renewable energy sources. The chapter sets the stage for the thesis by presenting the research goals, outlining the significance of DSSCs in addressing energy needs and justifying the importance of the research.

Then chapter 2 delves into the previous work done on DSSCs, particularly focusing on the different types of dyes used and the fabrication processes employed. It examines the existing literature and studies related to DSSCs to provide a comprehensive understanding of the advancements and challenges in the field. The chapter also highlights the development of novel materials for DSSCs, including alternative dyes, electrode materials, and electrolytes.

In Chapter 3, the theoretical framework and working principle of DSSCs are presented. This chapter includes a detailed explanation of the underlying principles of DSSCs, such as electron transfer, charge transport, and light absorption mechanisms. Mathematical calculations and models relevant to DSSC operation are discussed, providing a solid foundation for understanding the core concepts of DSSC functionality.

Chapter 4 describes the experimental setup and methodology used in the research. It outlines the apparatus, instruments, and materials utilized for the experiments conducted throughout the thesis. The chapter provides a comprehensive explanation of the experimental procedures, ensuring the reproducibility of the results. It includes details on sample preparation, and measurement techniques followed during the experimentation.

Chapter 5 focuses on presenting the results obtained from the experiments conducted in the study. The chapter includes graphical representations, images, and calculated data to present the findings effectively. The results are discussed in light of the research objectives, and the implications and significance of the obtained results are analyzed. Characterization techniques employed to evaluate the performance and properties of the DSSCs are discussed, along with the corresponding instruments used.

The final chapter of the thesis summarizes the entire research and provides a conclusive assessment of the findings. It highlights the key outcomes, discusses the implications of the research, and evaluates the extent to which the research objectives were achieved. Additionally, Chapter 6 offers insights into the future scope of the work, suggesting potential avenues for further research and development in the field of DSSCs. It provides recommendations for enhancing the performance, stability, and efficiency of DSSCs and explores the broader implications of the research in addressing energy challenges.

The scope of this work aims to provide a comprehensive understanding of the potential of alternative dyes in improving the design, fabrication, and performance of DSSCs. The project will contribute to the advancement of renewable energy technologies by identifying efficient and cost-effective approaches to enhance the performance of dye-sensitized solar cells.

## 2.7 Conclusion

This literature review chapter has provided a comprehensive examination of the use of natural dyes, metal-free dyes, inorganic dyes, and organometallic dyes as sensitizers for TiO2-based dye-sensitized solar cells (DSSCs). Through the literature review, it has been established that chemical dyes have been extensively studied and utilized as sensitizers for DSSCs. They offer a wide range of colors but they often involve complex synthesis processes and exhibit limited stability. Natural dye based on Agro-waste dye, on the other hand, has emerged as a promising alternative due to its abundance, low cost, and potential for sustainable production. Agro-waste dye represents a sustainable and environmentally friendly option that can contribute to the development of greener DSSC technologies.

The fabrication and experimental comparison of DSSCs using synthetic organic dye, acrylic dye, and agro-waste dye sensitizers will provide valuable insights into their respective performance characteristics. The literature review has provided a comprehensive analysis of previous studies related to dye-sensitized solar cells (DSSCs). By synthesizing and evaluating the existing research, this review has identified key gaps, controversies, and developments in the field. This knowledge will serve as a valuable foundation for the subsequent section, where we will delve into the overview of DSSCs, highlighting their principles, components, and performance parameters. This knowledge will aid in the selection of sensitizers based on specific application requirements, such as efficiency, stability, and availability of resources.

# Chapter-3
# Overview of DSSC

## 3.1 Introduction

Dye-sensitized solar cells, which have reached a milestone of 30 years since their inception, are currently receiving significant attention from researchers who are dedicated to unlocking their maximum capabilities. Over the past few years, DSSCs and dye-sensitized photo-electro chemical cells have undergone a resurgence, emerging as the leading technology for various specialized applications. The Sun is the largest and most abundant source of energy, providing approximately 173,000 terawatts (TW) of energy to the Earth each year [74]. To put it into perspective, the energy the Sun radiates in just one hour surpasses the global energy consumption for an entire year. Photovoltaic (PV) electricity generation has experienced rapid growth, with an average annual increase of over 34% in the past decade, making it the fastest-developing energy technology worldwide [75]. However, despite this remarkable progress, PV cells currently contribute only 1% to global energy production. The International Energy Agency (IEA) predicts a 50% rise in renewable electricity production from 2019 to 2025 [76]. This surge in the capacity of individuals and organizations to generate their energy presents both opportunities and challenges on a global scale. The market for distributed solar PV systems in residential, commercial, and industrial buildings is expected to gain a strong foothold, with estimated installed capacity nearly doubling to 320 GW by 2025. Silicon-based solar technology remains the most widely adopted in manufacturing. Although alternative technologies like GaAs or CIGS offer comparable efficiency in single-junction systems, they still face cost challenges due to manufacturing and material expenses. Third-generation photovoltaic devices, known as hybrid solar cells, utilize inexpensive and abundant raw materials with the potential for achieving high efficiencies [77].

In 1991, Michael Grätzel and his research group achieved significant development in solar cell technology known as the dye-sensitized solar cell (DSSC) or Grätzel cell [78]. This innovative approach offered a promising alternative to conventional inorganic p–n junction solar cells by utilizing molecular systems and nanoparticles to replicate the process of photosynthesis. The primary objective was to harness sunlight as a renewable, dependable, and cost-effective energy source. Although the injection of dyes into a single crystal semiconductor was first demonstrated by Gerischer in 1966 [79,80], it was Grätzel's introduction of a mesoporous semiconductor layer that truly revolutionized DSSC technology. In DSSCs, dyes play a crucial role in absorbing light, separating charges, and

Converting photons into electrons. These dyes are attached to mesoporous semiconductors, which solely function to collect the resulting free electrons and transfer them to the electrode as an electric current [81]. To complete the circuit, electrons circulate back into the system through a charge transport material that regenerates the dye molecules [82-84]. DSSC devices have exhibited remarkable energy efficiencies exceeding 13% when exposed to full sunlight [85]. Furthermore, they are based on affordable raw materials and employ straightforward production techniques [86,87]. However, concerns have been raised regarding the sealing of liquid junction solar cells [88-91].To address this, improvements in sealing strategies or the substitution of the liquid electrolyte with a solid charge transfer material will significantly impact the commercial viability of DSSCs [92-96].

## 3.2 Why DSSC over Conventional Solar Cells

The manufacturing of conventional silicon solar cells does have certain environmental and industrial impacts. Here are some key considerations:

### 3.2.1 Raw Material Extraction

The production of silicon solar cells involves the extraction of raw materials, including silicon, which is typically derived from quartz or silica. Mining and processing these raw materials can have environmental impacts, such as habitat destruction, soil erosion, and water pollution. Proper mining practices and environmental regulations can help mitigate these impacts.

### 3.2.2 Waste Generation

Silicon solar cell manufacturing generates waste materials, such as silicon scraps, sludge, and chemical residues. Proper disposal and treatment of these wastes are crucial to prevent environmental contamination. Recycling and reusing waste materials can help reduce the overall environmental impact.

### 3.2.3 Occupational Health and Safety

The manufacturing industry, including solar cell production, involves various occupational health and safety risks. Workers may be exposed to chemicals, high temperatures, and mechanical hazards. Implementing appropriate safety measures and providing proper training to workers is essential to ensure a safe working environment.

### 3.2.4 Emissions and Effluents

Manufacturing processes can release air emissions, such as volatile organic compounds and greenhouse gases, depending on the energy sources used and the efficiency of pollution control systems. Wastewater generated during the manufacturing process may contain chemical contaminants that require proper treatment before discharge.

## 3.3 Potentiality of DSSCs

Dye-sensitized solar cells offer several potential advantages that can contribute to their market share in solar energy:

### 3.3.1 Efficiency

DSSCs have demonstrated high power conversion efficiencies, with some reaching levels comparable to traditional silicon solar cells. Continued research and development efforts aim to further improve their efficiency, making them a competitive option in the solar energy market.

### 3.3.2 Versatility

DSSCs are highly versatile and can be fabricated on flexible substrates, enabling the production of lightweight, flexible, and even transparent solar modules. This versatility allows for various applications, such as integration into building facades, windows, or curved surfaces, expanding the possibilities for solar energy utilization.

### 3.3.3 Low-Light Performance

DSSCs exhibit excellent performance in low-light conditions, including indirect and diffused sunlight. This characteristic makes them particularly suitable for regions with less sunlight or during cloudy or overcast days, where traditional solar technologies may experience performance degradation.

### 3.3.4 Cost-Effectiveness

DSSCs can potentially offer cost advantages compared to traditional silicon solar cells. The materials used in DSSCs are generally less expensive, and their fabrication processes are simpler and require fewer energy-intensive steps. These factors can contribute to reducing manufacturing costs and making solar energy more affordable.

### 3.3.5 Environmental Benefits

DSSCs have a lower environmental impact compared to some other solar cell technologies. They can be fabricated using eco-friendly and non-toxic materials, reducing potential harm during manufacturing, operation, and end-of-life disposal. Additionally, their production processes consume less energy and generate fewer greenhouse gas emissions.

### 3.3.6 Durability and Reliability

DSSCs have demonstrated good long-term stability, with several studies showing their durability over extended periods of use. Advances in materials and device design have addressed some of the initial concerns regarding the stability of DSSCs, making them a viable option for long-lasting solar installations.

### 3.3.7 Rapid Prototyping and Customization

DSSCs offer the advantage of rapid prototyping and customization due to their flexible and scalable production processes. This enables faster development and adaptation of solar cell designs for specific applications or customer requirements, allowing for more tailored solutions.

By capitalizing on these potential advantages, DSSCs can gain a significant market share in the solar energy industry. Continued research, technological advancements, and commercialization efforts will play a crucial role in further enhancing their performance, cost-effectiveness, and overall competitiveness in the renewable energy market.

## 3.4 Light and Energy

In outer space, the solar spectrum closely resembles that of a black body with a temperature of 5778 K. It encompasses a wide range of wavelengths, spanning from X-rays to radio waves( refer to [97] Fig. 3.1). However, as sunlight travels through the Earth's atmosphere, certain portions of the spectrum, such as X-rays, filtered out, resulting in a modified solar spectrum reaching the Earth's surface. The path of light through the atmosphere is quantified as air mass (AM) [98]. To facilitate the comparison of photovoltaic devices developed by different manufacturers and research labs, a standardized reference spectrum was established. This reference spectrum, known as AM1.5 Global (AM1.5G), exhibits a combined power intensity of 1000 $W*m^{-2}$ (equivalent to 100 $mW*cm^{-2}$) and is widely employed for measuring the efficiency of solar cells [99,100]. The sunlight's irradiance, depicted in Figure 3.1 [101], represents the amount of energy per unit area per unit time for a specific wavelength of light, measured in $W*m^{-2}*nm^{-1}$. By integrating the spectral irradiance across all wavelengths, the overall irradiance in W m−2 can be obtained.

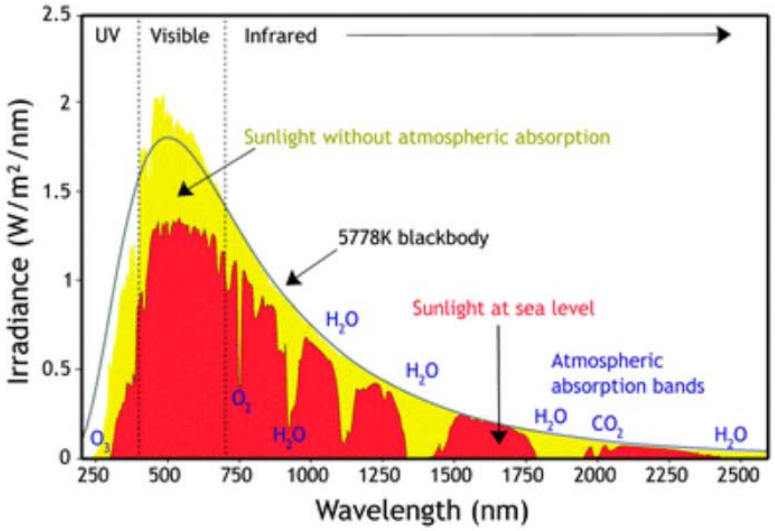


Figure 3.1 Solar irradiance spectrum

Dye-sensitized solar cells exhibit good performance when exposed to sunlight. However, their performance is even more impressive when illuminated by artificial light sources that emit a spectrum similar to the visible range of sunlight (refer to Figure 3.2 [107] ). This is evident in various studies [102-106]. It's important to note that indoor lighting conditions differ significantly from outdoor solar irradiance due to the substantially lower intensity of indoor light and the variations in spectra among different light sources. Typical indoor lighting has illuminance values ranging from 200 to 1000 lux (lux measures lumen per unit area, lm $m^{-2}$). In comparison, AM1.5G light has an illuminance value of approximately 100,000 lux, signifying the vast difference in intensity between indoor and outdoor lighting. Illuminance is a measure of light intensity as perceived by the human eye, whereas irradiance is a measure of energy. Converting illuminance to irradiance is not a straightforward mathematical operation because different light spectra can produce varying levels of irradiance at the same illuminance. For instance, a light bulb emitting blue light with an illuminance of 1000 lux will generate more irradiance compared to a bulb-emitting red light with the same illuminance. Determining the lamp spectrum is necessary before converting irradiance to illuminance using equation (3.1).

$$\mathrm{IL[lx]} = \frac{683.002}{A}\left[\mathrm{lm\ W^{-1}\ m^{-2}}\right]\int I(\lambda)\cdot E(\lambda)\left[\mathrm{J\ s^{-1}\ nm^{-1}}\right]\cdot \bar{y}(\lambda)\cdot \mathrm{d}\lambda \tag{3.1}$$

where IL is the illuminance, $I \cdot E$ is the irradiance (considering the area $A$ outside of the integral), given by the product of the light intensity $I$ and the photon energy $E$, and $\bar{y}$ is the dimensionless photo pic luminosity function of the human eye centered at about 555 nm.

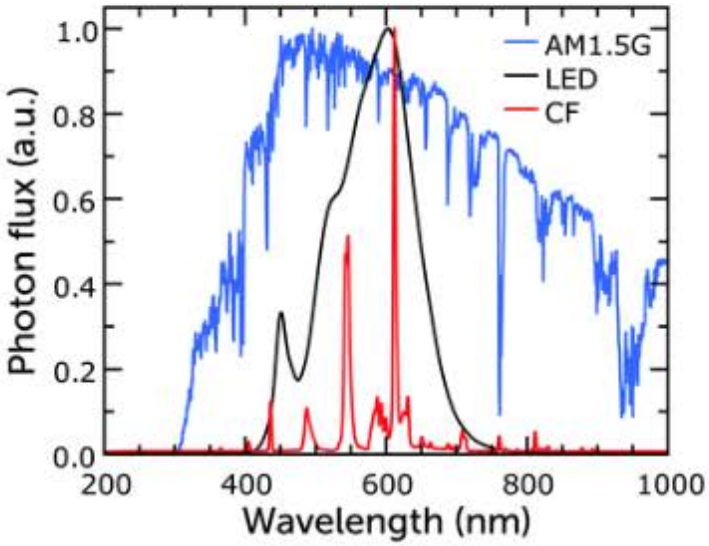


Figure 3.2 Normalized emission spectra of warm white fluorescent and LED bulbs, and of the AM1.5G standard

## 3.5 Operation & Structure

The fundamental components of a dye-sensitized solar cell consist of the dye-sensitized semiconductor electrode, the redox electrolyte, and the counter electrode. The absorption of light within the device is facilitated by a monolayer of dye molecules attached to the surface of the semiconductor. In traditional dye-sensitized solar cells, the semiconductor possesses an n-type characteristic, wherein electrons in the conduction band enable the electrical conductivity of the material. Moreover, the semiconductor has a wide bandgap and contributes minimally to the absorption of solar light. The most commonly utilized semiconductor in dye-sensitized solar cells is $TiO_2$ with the anatase crystal structure, which possesses a bandgap of approximately 3.2 eV and primarily absorbs UV light. For this discussion, $TiO_2$ will be assumed as the semiconductor, although it is worth noting that various semiconductors can be employed in dye-sensitized solar cells.

A flat and compact $TiO_2$ electrode with a monolayer of adsorbed dye fails to absorb sufficient light to achieve practically significant solar-to-electric conversion efficiencies. To capture a substantial portion of the solar spectrum, $TiO_2$ electrodes with high surface areas are utilized, such as the mesoporous $TiO_2$ electrode. This type of electrode consists of interconnected nanoparticles typically measuring around 20-30 nm in size. The electrode exhibits a porosity of approximately 50%, resulting in a surface area several hundred times greater than the projected area. Consequently, the quantity of adsorbed dye is also several hundred times greater compared to a flat surface. Dye molecules chemically bonded to the $TiO_2$ surface demonstrate superior performance in dye-sensitized solar cells. These molecules are also in contact with the redox electrolyte, which fills the pores of the mesoporous electrode. The redox mediator facilitates the transfer of positive charges to the counter electrode, which is commonly situated close to the working electrode, often in a parallel configuration. The technology of dye-sensitized solar cells (DSSC) distinguishes itself from conventional silicon solar cells not only in their physical construction but also in their working mechanism. The operation of DSSC bears similarities to the natural process of photosynthesis, with the dye playing the role of the light absorber, replacing chlorophyll. In this process, carbon dioxide is substituted by $TiO_2$, which acts as the electron acceptor. Oxygen serves as both the electron donor and the oxidation product. Instead of water, an electrolyte is utilized to regenerate the process, ensuring its sustainability. Additionally, DSSCs employ a multilayer structure designed to enhance both light absorption and electron collection efficiency, thereby maximizing overall performance.

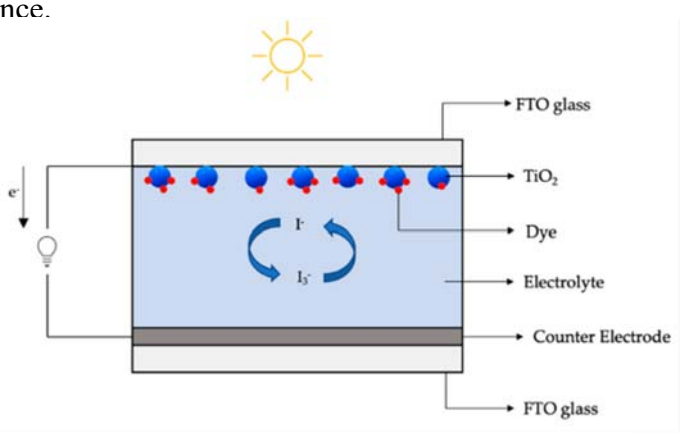


Figure 3.3 Basic Structure of DSSC

The Dye-Sensitized Solar Cells commonly adopt a standard structure referred to as the sandwich cell configuration. This configuration entails the placement of conducting glass

substrates, serving as both the working and counter electrodes, in a face-to-face orientation. The basic structure of DSSC is given in Figure 3.3 [112]. The electrodes are separated by a thin layer of redox electrolyte, as depicted in Figure 3.3. The photo-electrode, situated on the working electrode, comprises FTO glass coated with a mesoporous film of $TiO_2$ on its surface. This mesoporous layer plays a vital role in the DSSC operation as it serves as a host for the adsorption of a specific dye. The sensitizer dye, capable of capturing photons from incident light and initiating the electron injection process, is bound to the surface of the mesoporous semiconductor layer. By absorbing a wide range of wavelengths, the dye enables the transfer of excited electrons to the semiconductor material.

The electrolyte, situated between the photoactive layer and the counter electrode, is composed of a redox couple solution. This solution, typically in liquid or gel form, consists of a redox mediator and an electrolyte salt. The redox mediator plays a crucial role in regenerating the dye by accepting electrons from the photoactive layer, while the electrolyte salt enhances the ionic conductivity required for efficient charge transfer. The counter electrode, situated on the opposite side of the redox electrolyte, is composed of FTO glass coated with a catalyst material. Examples of catalysts commonly used include platinum nanoparticles, carbon, or conducting polymers. This counter-electrode configuration allows for (semi-)transparency, thereby enabling illumination from either side if the counter electrode possesses transparency.

The operation of DSSC is as follows based on the diagram Fig. 3.4 [(108]-[111]):

(i) Excitation of sensitizer: As pointed on Figure 3.2, when photons from sunlight fall on the surface of the DSSC, the sensitizer pumps up to a higher energy state (equation 3.2) [lowest unoccupied molecular orbital (LUMO)] from their inactive state [highest occupied molecular orbital (HOMO)] from step 1 to step 2 followed by equation1 and thereon generates electrons and holes.

$$S \xrightarrow{h\nu} S^* \tag{3.2}$$

(ii) Injection of the electron: The excited sensitizer is oxidized and an electron gets into the conduction band (CB) of the photo-anode semiconductor (e,g, $TiO_2$), whereby electrons pass through the thin film of porous $TiO_2$ to the transparent conducting oxide glass substrate. To the cathode from the anode through an external loop, producing current and

completing cycles followed by the equation the excited dye molecule ($S^*$) is oxidized (equation 3.3) and an electron is injected into the conduction band of the semiconductor. Electrons can now move freely as the semiconductor is conductive at this energy level.

$$S^* \longrightarrow S^+ + e^- \tag{3.3}$$

(iii) Regeneration of sensitizer: The redox pairs present in the electrolyte (iodide and triiodide [I- = I3 -] redox pairs) donate the electron to oxidized-sensitizer, and thus it gets regenerated. The oxidized dye molecules ($S^+$) are again regenerated by electron donation from the iodide in the electrolyte ref. to equation 3.4

$$S^+ + \frac{3}{2}I^- \longrightarrow S + \frac{1}{2}I_3^- \tag{3.4}$$

(iv) Electro-chemical reduction: In addition, iodide and the redox mediator in the electrolyte travel to the counter electrode and are regenerated on the cathode by reducing tri-iodide (equation 3.5).

$$\frac{1}{2}I_3^- + e^- \longrightarrow \frac{3}{2}I^- \tag{3.5}$$

Where S is the dye molecule and hv is the photon energy. Figure. 3.4 [113] explains the energy level diagram of DSSC. Figure 3.3. Describes the working schematic diagram of DSSC.

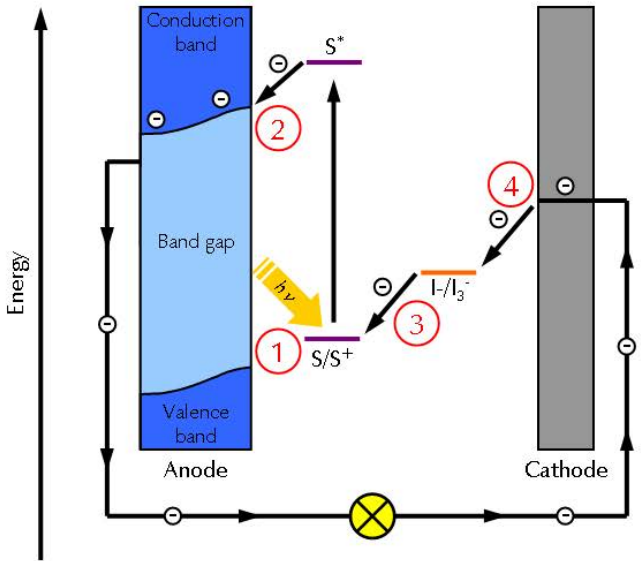


Figure 3.4 Energy level diagram of a dye solar cell

# 3.6 J-V Characteristics & Power Conversion Efficiency

Power conversion efficiency (PCE) is a critical parameter that determines the performance of a solar cell. It is obtained by analyzing the current density (J) versus potential (V) characteristics of the cell under illumination from a solar simulator. Standard measurements are conducted at 25 °C with 100 mW.cm$^{-2}$ light intensity and the AM1.5Gspectral distribution[114].

To record J-V curves, a source meter or potentiostat is used to apply controlled potentials to the device and measure the resulting current. Typically, voltage steps of 5 or 10 mV are applied, followed by a delay time of over 100 ms to allow the current to stabilize [115]. Insufficient delay time can lead to hysteresis, where the forward and reverse J-V curves differ. While hysteresis has been extensively discussed in perovskite solar cells, it has received less attention in DSSCs. Hysteresis in DSSCs is primarily caused by capacitive currents related to the charging or discharging of the mesoporous electrode [116] and mass transport in the electrolyte, resulting in concentration gradients of the redox couple [117].

The J-V curve provides several parameters: Jsc, the current density at zero applied potential, and Voc, the open-circuit potential at zero current. The maximum power point (MPP) occurs when the power output of the device (J multiplied by V) reaches its maximum, known PMPP. The fill factor (FF) is the ratio of PMPP (Figure 3.5) to the product of Voc and Jsc. A higher FF value (closer to 1) indicates a more square-shaped curve and signifies the ability of the solar cell to simultaneously deliver current and potential. The PCE is calculated using equation 3.6, where Plight represents the power density of the incoming light.

$$\mathrm{PCE} = \frac{P_{\mathrm{MPP}}}{P_{\mathrm{light}}} \times 100\% = \frac{V_{\mathrm{OC}} J_{\mathrm{SC}} \mathrm{FF}}{P_{\mathrm{light}}} \times 100\% \tag{3.6}$$

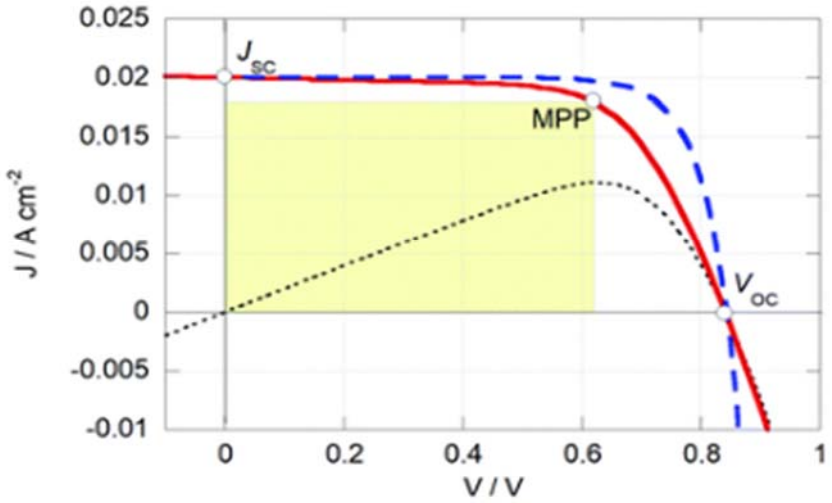


Figure-3.5 J-V Characteristics

To accurately, calculate the power conversion efficiency of a solar cell device, it is important to determine the active area of the device with precision. In the field of DSSCs, the most reliable method involves placing a black metal mask with an aperture directly on top of the solar cell. The area of this aperture is used for the PCE calculation, while any light entering from the sides is blocked to prevent outside light from affecting the measurement. The aperture area should be similar to or smaller than the DSSCs working electrode [44]. If a small aperture is used, a portion of the DSSCs remains unilluminated. However, this has minimal impact on the measured PCE as the non-illuminated areas generally do not contribute significantly to recombination current. It is also useful to record the J–V curve in the dark, without using the aperture area, for further analysis of the solar cell and accurate assessment of the measured working electrode area.

The general shape of the J–V curve of a DSSC can be adequately described by the Shockley diode equation with additional resistive losses, as shown in equation 3.7

$$V = \frac{nk_BT}{e}\ln\left(\frac{J_{ph}-J}{J_s}-\frac{V-JR_s}{J_sR_p}+1\right)-JR_s \qquad (3.7)$$

where n is the diode quality factor, kB is the Boltzmann constant, T is the absolute temperature, Jph is the generated photocurrent density, Js is the reverse bias saturation current density, and Rs and Rsh the series and shunt resistances (units: $\Omega/cm^2$), refer to Figure 3.6 and equation-3.7

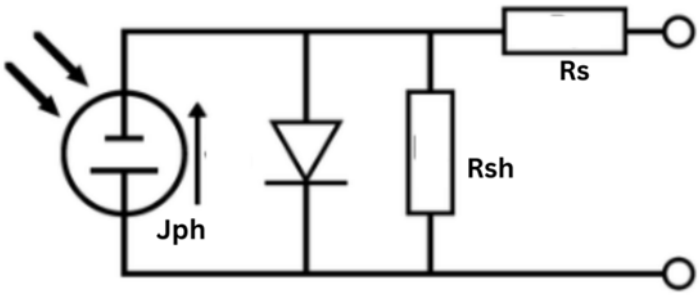


Figure 3.6 Equivalent circuit of DSSC

# 3.7 Incident photon-to-current conversion efficiency (IPCE)

During an IPCE measurement, the solar cell exposes to monochromatic light, typically generated by passing white light through a monochromatic. The short-circuit photocurrent is then recorded as a function of the light's wavelength. The IPCE is calculated using equation 3.8 and is usually plotted as a spectrum known as the photocurrent action spectrum.

$$\mathrm{IPCE}[\%] = \frac{1240}{\lambda[\mathrm{nm}]} \times \frac{J_{SC}[\mathrm{A\ cm^{-2}}]}{P_{\mathrm{light}}[\mathrm{W\ cm^{-2}}]} \times 100\% \tag{3.8}$$

In the equation, λ represents the wavelength of the incident light, and Plight refers to the power density of the light. IPCE measures using either DC or AC methods. In the DC method, only monochromatic light is used, while in the AC method, chopped monochromatic light is applied, and constant white light may be added. The AC photocurrent response is measured using a lock-in amplifier. Both methods should yield similar results, assuming that the photocurrent scales linearly with light intensity and that the chopping frequency in the AC mode is sufficiently low.

## 3.8 Conclusion

This chapter provided a comprehensive overview of the theory, operations, structure, and characteristics of Dye-Sensitized Solar Cells (DSSCs). We began by delving into the fundamental theory behind DSSCs, highlighting their characteristics and methods for harnessing solar energy. The concept of light absorption by sensitizing dyes and subsequent charge transfer processes is explained in detail. This theoretical foundation helped establish the basis for understanding the working principles of DSSCs.

Moving on to the working principle, we explored the systematic operation of DSSCs with equivalent circuits. The structure of a typical DSSC, comprising a transparent conductive substrate, a photoactive layer, an electrolyte, and a counter electrode, is thoroughly discussed. The interplay of these components and their role in facilitating the conversion of light energy into electrical energy are elucidated. The key processes involved, including light absorption, electron injection, electrolyte regeneration, and charge collection, are described comprehensively.

The knowledge guided us to the design and development of the experimental setup and methodology, ensuring accurate and reliable data collection. By aligning the experimental procedures with the fundamental understanding of DSSCs, this research aims to contribute to the advancement of this promising solar cell technology.

# Chapter-4
# Experimental Setup & Methodology

# 4.1 Introduction

The experimental setup and methodology chapter provides a comprehensive description of the procedures and equipment used in the fabrication of DSSCs. This section outlines the step-by-step process involved in creating the DSSCs, from the preparation of materials to the assembly and testing of the final device. By detailing the experimental setup and methodology, this chapter serves as a guide for researchers and technicians interested in replicating or modifying the fabrication process. The experimental setup for dye-sensitized solar cell fabrication typically includes various equipment and tools necessary for substrate preparation, film deposition, sensitization, counter electrode preparation, and cell assembly. The following sections provide a comprehensive description of the major components used in the cell assembly and their fabrication methods.

Table 4.1 Material List

| Sl | Material Name | Speciations | Manufacturer |
|---|---|---|---|
| 1. | Fluorine-doped Tin Oxide Glass | Size: L25 mm x W 25mm x T 2.2mm. Resistivity: 15 ohms/sq | Shilpent, Shilpa Enterprises |
| 2. | Titanium di-Oxide powder | Type: Rutile, Purity: 98%, Density: 3.78 g/cm. Molar mass: 79.866 g/mol | Swastik Interchem Pvt. Ltd. |
| 3. | Ethyl Alcohol | Purity: 99.99%, Lab grade | Generic |
| 4. | Acetone | Purity: 99% | Merck Specialities Pvt. Ltd. |
| 5. | Potassium iodide | pH: 6-9.2, Molar mass: 166 g/mol | Merck Life Science Pvt. Ltd. |
| 6. | Iodine resublimed | Molar mass- 253.80 g/mol, | Merck Life Science Pvt. Ltd. |
| 7. | Ethylene Glycol | Melting point: -58 degree Celsius, Evaporation rate- 5, Density- 0.86g/cm3. | Loba Chemie Pvt. Ltd. |
| 8. | Triton X | pH: 6-8 | Loba Chemie Pvt. Ltd. |
| 9. | Methyl Violet | Powder form, Melting point- 137 degree Celsius, Soluble in water | Loba Chemie Pvt. Ltd |
| 10. | Fabrica Acrylic Colour | | Camel |

## 4.2 Experimental Apparatus

### 4.2.1 Magnetic Stirrer

The magnetic stirrer (Figure 4.1) is used to process the smooth $TiO_2$ paste at room temperature. This is manufactured by REMI and input wattage is around 160W only for the stirrer part of the instrument.


Figure 4.1 Magnetic Stirrer

### 4.2.2 Piezo-U-Sonic Ultrasonic Cleaner

This ultrasonic cleaner (Figure 4.2) is used to ensure the complete cleanness of Fluorine-doped Tin Oxide (FTO) glass substrates. The input power is around 120W.


Figure 4.2 Piezo-U-Sonic Ultrasonic Cleaner

## 4.2.3 Analytical Balance Machine

The digital analytical balance machine (Figure 4.3) has a high level of precision and readability, allowing r to weigh small quantities of chemicals with great accuracy. With its advanced digital features and calibration capabilities, the digital analytical balance machine ensures reliable and reproducible results in various laboratory applications.

Figure 4.3 Analytical Balance Machine

## 4.2.4 Air Oven

The air Oven (Figure 4.4) utilizes heated air circulation within a chamber to maintain a consistent and precise temperature, ensuring uniform heat distribution and efficient drying of the substances being tested. It is used to facilitate accurate and reproducible experimental procedures for allowing samples to be dried, heated, or annealed.


Figure 4.4 Air Oven

## 4.2.5 Muffle Furnace

The muffle furnace (Figure 4.5) provides controlled heating in an enclosed chamber, allowing for precise temperature regulation and uniform heating of samples. The muffle furnace is commonly used for tasks such as ashing, calcination, and heat treatment,


Figure 4.5 Muffle Furnace

## 4.2.6 Solar Power Meter

The TES 1333 solar power meter (Figure 4.6) is used for radiation measurement on the horizontal surface level of the module surface. In this instrument range of irradiation, measurement is up to 2000 w/m2 with a spectral response of 400-1100 nm with an accuracy of ±10 w/m2.


Figure 4.6 Solar Power Meter

### 4.2.7 Data Logger

Agilent 34970A data acquisition system (Figure 4.7) is used for continuous data monitoring and recording of PV characteristics with different conditions. The instrument was logged and stored data every second.


Figure 4.7 Data Logger

## 4.3 Experimental Procedure

### 4.3.1 Cleaning the FTO Glass Substrates

In the initial stage of the DSSC fabrication process, cleaning of the Fluorine-doped Tin Oxide Glass (FTO) glass substrates is essential to ensure the removal of any impurities. This step is crucial for achieving optimal performance and reliable results. The FTO glass substrates are initially immersed in DI water, which acts as a gentle cleansing agent. This helps in dislodging and dissolving any loose particles or residues on the substrate's surface. The substrates are gently agitated in the DI water. Following the initial DI water cleaning, the FTO glass substrates undergo an additional cleaning step. They were immersed in a beaker containing a mixture of ethanol and acetone solution in a ratio of 3:1.(Figure 4.8) The beaker was then placed inside a chemical bath chamber (Figure 4.9), with the heater set to a temperature of 160°C for 2.30 hours. The chemical bath chamber was connected to an ultrasonic cleaner (Figure 4.10). This combination of solvent immersion, controlled temperature, and ultrasonic agitation ensures thorough cleaning and removal of contaminants from the FTO glass substrates. The entire

setup provides the best way to clean the FTO glass substrate. Ethanol is a commonly used solvent that effectively removes organic residues and provides a clean surface for subsequent processing steps and Acetone is a powerful solvent that helps in the removal of stubborn contaminants, such as adhesive residues or grease. The substrates are immersed in a beaker containing the solution and gently to facilitate the cleaning process.

Figure 4.8 Ethanol &Acetone Solutions

Figure 4.9 Chemical bath chamber


Figure 4.10 Ultrasonic Cleaner setup

## 4.3.1.1 Drying the Substrates

After the cleaning process, it is crucial to ensure that the FTO glass substrates are completely dry before proceeding to the next fabrication steps. Excess moisture can negatively affect subsequent layers and their adhesion. To dry the substrates, they were

placed in an air oven set at a temperature of 55°C. The controlled heat facilitates the evaporation of any remaining liquid, ensuring a dry and clean surface.

The thorough cleaning of FTO glass substrates through a multi-step process using DI water, the solution of ethanol and acetone, followed by controlled drying, provides a clean and pristine surface for subsequent deposition and fabrication steps in DSSC fabrication. This meticulous cleaning procedure ensures the removal of impurities and enhances the overall performance and reliability of the fabricated solar cells.

## 4.3.2 Preparation of $TiO_2$ Paste

Electrodes play a crucial role in the assembly of dye-sensitized solar cells (DSSCs), as they contribute to the overall performance of the device. The performance of a DSSC relies on the interaction between the dye and semiconductor electrodes, which act as sensitizers. In a DSSC, three simultaneous processes occur. Firstly, the dye molecules are absorbed into the $TiO_2$ layer of the electrode, where they interact with sunlight and release an electron from the atomic structure's lower orbit to an excited state (see the structure of DSSCs). This photoexcitation process is facilitated by the photons from the sunlight entering the DSSC. Secondly, there is the diffusion of electrons into the titanium dioxide layer. In the initial step, a chemical glass jar was used to measure 3 grams of $TiO_2$ powder. Then this powder was mixed with a solution consisting of ethanol and deionized water in a ratio of 5:5 with two drops of Triton X. Utilizing a magnetic stirrer at room temperature and a stirring speed of 470 rpm (Figure 4.11), the mixture was stirred for 2 hours, as illustrated in the figure 4.11. This stirring process effectively eliminated any lumps and resulted in a smooth $TiO_2$ paste, which was subsequently deposited onto the FTO (Fluorine-doped Tin Oxide) glass substrate.


Figure 4.11 Preparation of $TiO_2$ paste

## 4.3.3 Preparation of Dyes

## 4.3.3.1 Methyl Violet Dye

In the laboratory, we began by obtaining methyl violet powder (Figure 4.12) and a petri dish. methyl violet is an organic dye, the chemical structure is given in Figure 4.13. Using a precise weighing machine, we measured 0.04g of methyl violet powder and carefully transferred it into the petri dish (Figure 4.14). Next, we take a clean glass rod and use it to dilute the powder by stirring it with 20 ml of deionized water at room temperature. The petri dish, as illustrated in the accompanying figure, serves as the container for this mixture. This process ensures that the methyl violet powder is uniformly dispersed in the water, allowing for accurate experimental procedures to be carried out.


Figure 4.12 Methyl Violet Powder

Figure 4.13 Solution of Methyl Violet

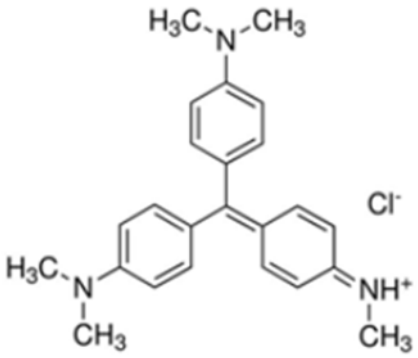


Figure 4.14 Chemical Structure of Methyl Violet

## 4.3.3.2 Acrylic Colour-Dye

Here we have taken fabric acrylic color (Figure 4.15), which mostly use in the painting and textile industries. This is a composite material, that contains pigment, polymer binder, additives, and water. To prepare an acrylic Prussian blue dye solution (Figure 4.16) for the TiO2 electrode, stated by purchasing commercial acrylic Prussian blue color from a shop, along with a petri dish from a lab. Using a weight machine, measured 3g of acrylic paste and transferred it to the petri dish. Diluted the paste with 15 ml of deionized (DI) water using a clean glass rod. This process, determined through trial and error, yields the best results for the TiO2 electrode to effectively absorbed the acrylic dye

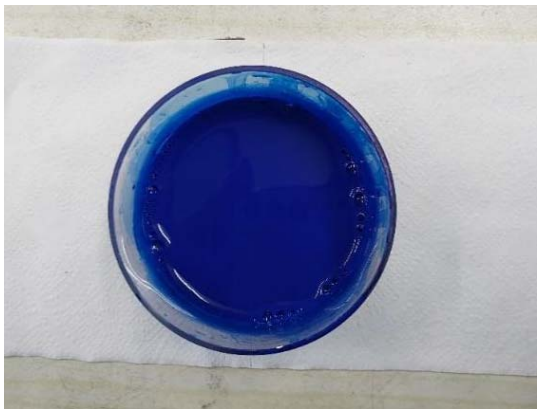

Figure 4.15 Solution of Acrylic Colour


Figure 4.16 Prussian blue Acrylic Colour

## 4.3.3.3 Agro-waste Dye

Bougainvillaea flowers collected from the campus. From those flowers manually we collected only bracts as samples. These bracts contain Betacyanins pigment, a chemical structure with an anchor group pointed out in Figure 4.19, which absorbs UV and the visible range of the spectrum. The first step involved measuring the weight of the sample using a weight machine, and it was found to be 4.4 grams. To eliminate any impurities, the bracts are thoroughly cleaned with deionized (DI) water, repeating the rinsing process 2-3 times. After cleaning, the sample was placed on tissue paper to reduce its water content (Figure 4.16). Subsequently, they dried using an air oven at a temperature of 35 degrees Celsius for 5 minutes. To create a solution, acetone and ethanol were mixed in a ratio of 4:6. Then the dried sample was immersed in this mixture and left to rest for 24 hours. After this duration, the extraction was obtained from the sample, which is depicted in Figure 4.17.

To preserve the dye, it was stored in a freezer at a temperature of -10 degrees Celsius. At the end of the 30 days, the dye obtained, and its appearance are represented in Figure 4.18. End of the 30 days, the cell was fabricated with the preserved dye (as shown in Figure 4.18).

The significance of this process lies in the utilization of bougainvillea bracts, which are commonly considered agro-waste and not typically utilized. The entire process developed through trial and error, and it was found to be particularly effective for the absorption of tio2 electrodes.

Figure 4.17 Cleaned Bougainvillea Bracts

Figure 4.7 Fresh Extracted Solution

Figure 4.18 After 30days of extraction

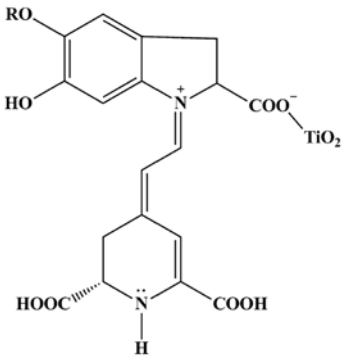


Figure 4.19 Chemical Structure of Betacyanins molecules.

## 4.3.4 Electrolyte preparation

The next step in assembling a Dye Sensitized Solar Cell involves preparing the electrolyte, which plays a critical role in the cell's functionality. The electrolyte acts as a medium for

transporting charges between the electrodes, enabling the movement of charge carriers within the cell. It also serves to replenish the dye and itself continuously, contributing to the stability and performance of DSSCs and enhancing their solar-to-electric conversion efficiency.

For liquid-based electrolyte DSSCs, the solution is prepared by dissolving 0.127 grams of iodine crystal ($I_2$) and 0.83 grams of potassium iodide (KI) in 10 ml of ethylene glycol. Then this solution was stirred at room temperature and kept in a dark container for 72 hours, as shown in Figure 4.20. Once the components are thoroughly mixed, the electrolyte solution is stored in a dark position, such as a drawer, at room temperature. The resulting liquid-based electrolyte is then utilized in the fabrication of the DSSC.

Figure 4.20 Electrolyte solution stored in a dark container

## 4.3.5 Counter Electrode Preparation

The last step in assembling the Dye-Sensitized Solar Cell involves the preparation of the counter electrode through carbon coating, as depicted in the figure. To achieve this, the FTO substrate was placed over the burning flame of a candle (Figure 4.21). A layer of carbon formed on the substrate, which served as the counter electrode for the DSSCs. This carbon coating process is highly efficient, readily accessible, and cost-effective.

Figure 4.21 Process of Carbon layer

## 4.4 The assembly process of the DSSC

- **Step 1:** The FTO glass substrate is carefully cleaned and prepared for the deposition process. It is rubbed with soft tissue paper to ensure cleanliness (Figure 4.22).

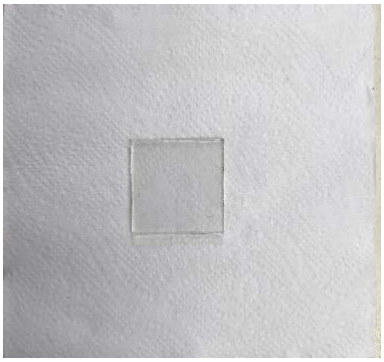

Figure 4.22 Cleaned FTO glass substrate

- **Step 2:** A prepared TiO2 paste is deposited onto the FTO substrate using the doctor blade method. The paste spread evenly on the substrate to create a uniform TiO2 layer (Figure 4.23).


Figure 4.23 Process of $TiO_2$ layer using doctor blade method

- **Step 3:** After the deposition, the $TiO_2$ layered FTO glass substrate was allowed to dry naturally and then annealed in a muffle furnace at a temperature of 330 degrees Celsius for 2 hours (Figure 4.24). This annealing process helps to enhance the structural integrity of the $TiO_2$ layer.

Figure 4.24 Heat treatment of $TiO_2$ layer inside the Muffle Furnace

- **Step 4:** Once the annealing process was complete, the photo-electrode was removed from the furnace and cooled to room temperature naturally. Then the photo-electrode was immersed in a petri-dish, containing diluted dye, ensuring complete coverage. The petri dish was kept in a dark position at room temperature for 24 hours to allow for the dye sensitization of the $TiO_2$ layer.

- **Step 5:** After the 24-hour sensitization period, the photo-electrode was taken out from the petri dish, and excess dye was removed by rinsing with deionized (DI) water. The rinsed photo-electrode was then dried using an air oven at a temperature of 40 degrees Celsius for 5 minutes to ensure the complete removal of moisture. Here are the Figures of Photo-electrode with the corresponding dye (Figure 4.25).

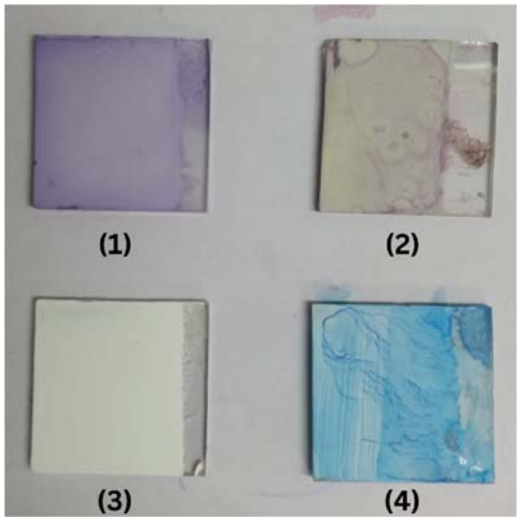


Figure 4.25 (1) Methyl Violet (2) Bougainvillea Brac (3) $TiO_2$ layer (4) Acrylic Colour

- **Step 6:** A different FTO substrate is positioned above the open flame of a candle to generate a carbon layer as a counter-electrode (Figure 4.26). On the other hand, we got a photoanode. Now both electrodes were ready to be processed further (As shown in Figure 4.27)


Figure 4.26 Carbon layer on FTO

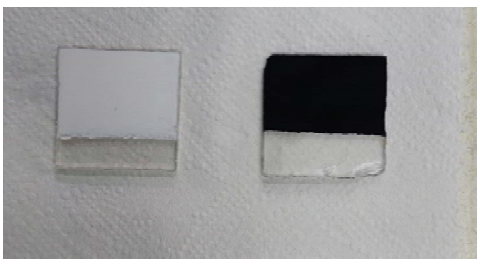

Figure 4.27 Photo-anode and Counter Cathode

- **Step 6:** In the final step, a single drop of the prepared liquid-based electrolyte is placed on the sensitized photo-electrode (Figure 4.28). The counter-electrode was then aligned and placed on top of the front photo-electrode, and the two electrodes were securely combined using a binder clip.

This assembly process was repeated for three different dye-based DSSCs, following the same steps for each cell (Figure 4.29).

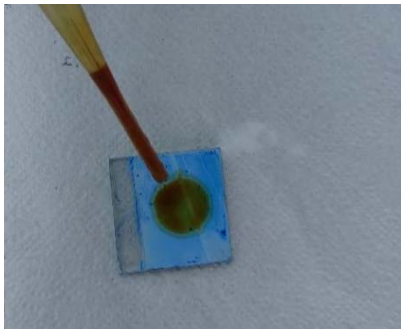

Figure 4.28 Single drop of prepared electrolyte solution on Photo-anode with dye

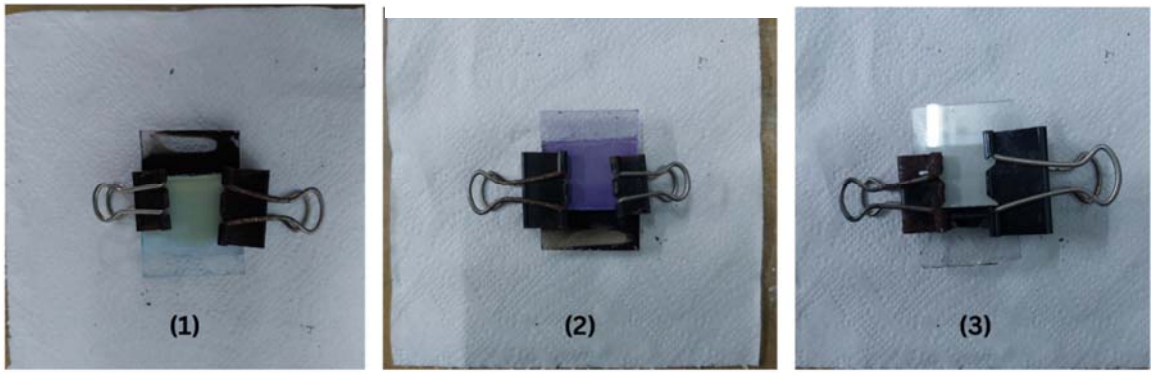


Figure 4.29 Fabricated DSSCs (1) Acrylic colour (2) Methyl Violet (3) Agro-waste

# 4.5 Conclusion

The primary aim of this chapter was to investigate and enhance the fabrication process of dye-sensitized solar cells to achieve improved efficiency and reliability. A key focus is placed on the preparation of materials and the fabrication process, starting with the meticulous cleaning and preparation of FTO glass substrates, ensuring their suitability for the subsequent assembly process. To summarize, this experimental study delved into the assembly process of DSSCs, offering comprehensive insights into the materials, types of

machinery, and preparation techniques employed. The methodology adopted ensured the precise fabrication of DSSCs, resulting in optimized performance. The systematic assembly process encompassed crucial steps such as cleaning, deposition, annealing, sensitization, rinsing, drying, and electrode combination, all of which were successfully executed.

The process followed by Chapter 5, where the utilization of appropriate characterization techniques in this research allows for the comprehensive analysis of key performance parameters and material properties. By following the experimental setup and methodology, with the obtained results and subsequent discussion, this study aims to provide valuable insights and contribute to the understanding and improvement of DSSCs.

# Chapter 5
# Characterization Techniques, Results & Discussion

## 5.1 Introduction

The field of renewable energy has gained significant attention in recent years due to the increasing demand for sustainable and clean energy sources. Among various renewable energy technologies, dye-sensitized solar cells (DSSCs) have emerged as a promising alternative to traditional silicon-based photovoltaic devices. DSSCs offer several advantages, including low production costs, ease of fabrication, and the ability to harness energy even under low light conditions. In this study, we present an explorative investigation focused on comparing the performance of alternative dyes in DSSCs. We employed a comprehensive characterization approach, which involved various analytical techniques, namely scanning electron microscopy (SEM), X-ray diffraction (XRD), spectrophotometry analysis, and current-voltage (J-V) characteristics measurement. By utilizing these techniques, we aimed to gain insights into the morphological, structural, optical, and electrical properties of DSSCs.

Through this comprehensive study, we aim to compare the alternative dyes used in DSSCs and evaluate their performance based on various characteristics, compare the various dye based DSSCs The findings of this study will contribute to the understanding of the factors influencing the efficiency of DSSCs and aid in the development of more efficient and cost-effective solar cell technologies.

## 5.2 Characterization Techniques

### 5.2.1 X-ray powder diffraction

Max von Laue made a significant discovery in 1912 when he found that crystalline substances act as three-dimensional diffraction gratings for X-ray wavelengths, similar to the spacing of planes in a crystal lattice. This discovery led to the development of X-ray diffraction as a common technique for studying crystal structures and atomic spacing.

X-ray powder diffraction (XRD) is a widely used analytical technique that helps quickly identify the phases present in crystalline materials and determine their unit cell dimensions. It provides valuable information about the arrangement of atoms within crystals.

The underlying principle of XRD involves the constructive interference of monochromatic X-rays with a crystalline sample. Monochromatic X-rays are generated using a cathode ray tube, and their wavelength is filtered to produce radiation of a specific wavelength. The X-rays are then collimated to concentrate them and directed toward the sample. When these incident X-rays interact with the crystal, they undergo constructive interference, leading to the formation of diffracted rays. This diffraction phenomenon occurs when the conditions described by Bragg's law are met.

Bragg's law can be expressed as:

$$n\lambda = 2d \sin \theta \quad (5.1)$$

In this equation 5.1, λ represents the wavelength of the X-rays, d denotes the interplanar spacing within the crystal lattice, θ corresponds to the X-ray angle, and n is an integer. Bragg's law establishes a relationship between the X-ray wavelength, the diffraction angle, and the lattice spacing in the crystalline sample. The diffracted X-rays are then detected, processed, and counted.

To explore all possible diffraction directions of the crystal lattice, the sample is scanned through a range of 2θ angles. This is accomplished by taking advantage of the random orientation of powdered materials. By converting the resulting diffraction peaks into d-spacings, it becomes possible to identify the mineral or phase present in the sample. Each mineral or phase has its own unique set of d-spacings, which can be compared to reference patterns for identification.

X-ray diffraction techniques rely on the generation of X-rays using an X-ray tube. These X-rays are directed toward the sample, and the resulting diffracted rays are collected. The angle between the incident and diffracted rays plays a crucial role in all diffraction experiments. While there may be variations in instrumentation between powder and single-crystal diffraction, the fundamental principle remains the same [118].

In our project, the primary objective of the XRD analysis is to determine the type of semiconductor layer (TiO2) and its crystallinity. The results obtained from the XRD graph will be discussed in the subsequent section of this chapter. Figure 5.1 represents the XRD Machine.

Figure 5.1 Instrument of XRD

## 5.2.2 Scanning Electron Microscopy

Scanning Electron Microscopy is a powerful imaging technique that uses a focused beam of electrons to generate high-resolution, three-dimensional images of the surface of a sample. It provides detailed information about the sample's morphology, topography, and composition. Using conventional SEM techniques, areas ranging from approximately 1 cm to 5 microns in width can be imaged in a scanning mode, with magnification ranging from 20X to approximately 30,000X and a spatial resolution of 50 to 100 nm.

The accelerated electrons in an SEM possess significant kinetic energy, which is dissipated through interactions with the sample, resulting in the production of various signals. These signals include secondary electrons (used to create SEM images), backscattered electrons (BSE), diffracted backscattered electrons (EBSD, employed for determining crystal structures and orientations), photons (characteristic X-rays used for elemental analysis and continuum X-rays), visible light (cathode luminescence--CL), and heat. Secondary electrons are particularly useful for imaging samples as they reveal morphology and topography, while backscattered electrons are effective in illustrating composition contrasts

in multiphase samples, enabling rapid phase discrimination. X-ray generation occurs due to inelastic collisions between incident electrons and electrons in discrete orbitals (shells) of atoms within the sample. As the excited electrons return to lower energy states, they emit X-rays of fixed wavelengths that are characteristic of specific energy level differences between electron shells for a given element. Therefore, characteristic X-rays are produced for each element present in a mineral when it is "excited" by the electron beam. Notably, SEM analysis is considered non-destructive as the generation of X-rays from electron interactions does not result in volume loss of the sample, allowing for repeated analysis of the same materials [119,120].

In the following section, we have presented a comprehensive analysis of the SEM, focusing on the particle size and shape of both electrodes. Visual representations from the Inspect f50 model (Figure-5.2) in the form of appropriate images are included to support our findings.


Figure 5.2 Instrument of SEM

## 5.2.3 Spectrophotometry

Spectrophotometry is a widely used method for quantifying the absorption of light by a chemical substance. It involves measuring the intensity of light as it passes through a sample to determine the extent to which the substance absorbs or transmits light across a range of wavelengths. This technique is valuable in various fields, including chemistry,

physics, biochemistry, material and chemical engineering, and clinical applications, for quantitative analysis.

Spectrophotometry is based on two fundamental laws: Lambert's law an d Beer's law. According to Lambert's law, the amount of light absorbed is directly proportional to the thickness (length of the light path) of the solution being analyzed. The equation is expressed as $A = \log10(I_0/I) = as * b$, where $I_0$ represents the incident light intensity, “I” is the transmitted light intensity, as is the absorbency index characteristic of the solution, b is the thickness of the medium, and A is the absorbance.

Beer's law states that the amount of light absorbed is directly proportional to the concentration of the solution. The equation is expressed as $A = \log10(I_0/I) = as * c$, where c represents the concentration of the solution. By combining the two laws, the equation becomes $A = \log10(as * b * c)$. In spectrophotometers, the internal diameter or width of the cuvette is typically maintained at exactly 1 cm to simplify calculations.

After passing through the solution, the light energy received at the phototube is expressed as percent transmittance (% T). By comparing this with the intensity of light at the source, the amount of light absorbed (not transmitted) can be measured. This is represented by the equation $I/I_0 * 100 = \%T$, where I is the light that passes through the sample, and $I_0$ is the intensity of light at the source. The absorbance (A) is calculated using the equation $\log10(I/I_0)$. By measuring the absorbance or transmittance, it is possible to determine the concentration of the absorbing molecule in the solution. If the molar absorptivity of the molecule (the amount of light absorbed at a specific wavelength by a specified concentration of solute in moles/liter) is known, the concentration can be directly calculated [121,122].

In this project, the dye plays a crucial role as it absorbs the solar spectrum, which is then converted into electricity. To determine the absorbance spectrum range for various dyes used in DSSCs (Dye-Sensitized Solar Cells), Spectrophotometry is employed with the Lambda 35 UV/VIS Spectrometer manufactured by Perkin Elmer(Figure 5.3). The details of the Spectrophotometry analysis will be discussed in the subsequent chapter, specifically in the section dedicated to Spectrophotometry analysis.

Figure 5.3 Spectrometer

## 5.2.4 I-V Characteristics

Figure 5.5 shows the I-V characteristics of a diode and a solar cell. The total current ($I_L$) due to illumination is the sum of these two currents. In the study of photovoltaic cells, it is common to consider $I_L$ as a positive quantity by changing the polarity references. we can express it as:

$$I=I_L - I_D \qquad (1)$$

This equation represents the characteristic equation of the solar cell(Figure-5.6). Based on the equivalent circuit of a solar cell, the mathematical equation can be modeled using a single exponential term:

$$I = I_L-I_0 * [\exp((eV/mkT)-1] \qquad (2)$$

Here, e represents the charge of an electron, k is the Boltzmann constant, $I_{L0}$ is a constant, V is the voltage, I is the current, and T is the temperature. The equation (3) derived earlier expresses the short-circuit current (Isc) as:

$$I_{sc} = I_L = I=0 \qquad (3)$$

When the device is in an open circuit, the voltage reaches its maximum value, denoted as Voc, in the generation region. In open-circuit conditions, the photocurrent is completely compensated by the polarization current. This can be expressed by incorporating Equation (2) into Equation (4):

$$V_{oc} = (mkT/e) * [\ln( I_L/I_0)+1] \quad (4)$$

To create a more realistic model, two additional elements should be considered: the series resistance (Rs) and the parallel resistance (Rp), which impact the efficiency of the cell. The series resistance (Rs) represents the internal resistance caused by factors like the semiconductor's inherent resistance. In practice, all these resistant losses are typically represented by the solar cell's series resistance.

On the other hand, the parallel resistance (Rp) arises due to imperfections in the quality of the p-n junction and leads to current leakage The mathematical expression that relates current and voltage, taking into account these resistances, can be expressed as:

$$I = I_L - I_D$$
$$I = I_L - I_0\left[\exp\left(\frac{e(V+R_sI)}{mkT}\right)-1\right]-\frac{V-R_sI}{R_p} \quad (5)$$

Based on this theory the schematic diagram (Figure 5.4) is given below by which sample DSSCs were tested.

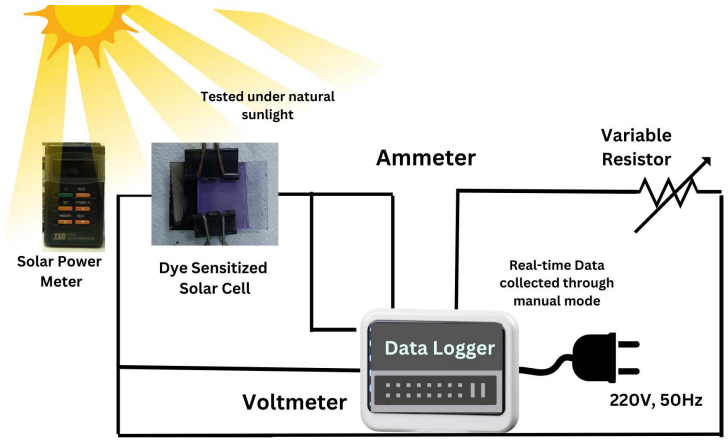


Figure 5.4 Schematic Diagram of Experimental Setup

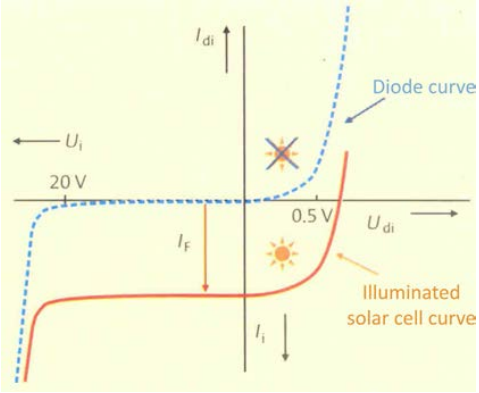


Figure 5.5 I-V curves of a diode and an illuminated photovoltaic Cell

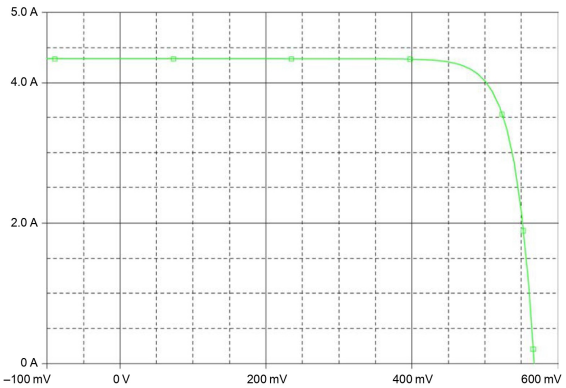


Figure 5.6 I-V curves of a Solar Cell

## 5.3 Scanning Electron Microscopy (SEM) Analysis

SEM analysis allows for the examination of the surface morphology and microstructure of the fabricated DSSCs. By observing the surface features, we assess the uniformity and distribution of the dye molecules, which play a crucial role in light absorption and charge transfer processes within the solar cell. Furthermore, SEM analysis enables the identification of any potential defects or irregularities that may affect the overall performance of the DSSCs.The SEM analysis was conducted to investigate the morphological characteristics of $TiO_2$ and carbon particles.

### 5.3.1 $TiO_2$ Particles

The SEM images of $TiO_2$ particles reveal a predominantly spherical morphology with a narrow size distribution. The particles exhibit a smooth surface and uniform shape, as observed in Figures 5.7(a), 5.7(b), 5.7(c), and 5.7(d). The elongated carbon particles display lengths ranging from 1 to 10 µm. The average particle size is determined to be approximately 250 nm.

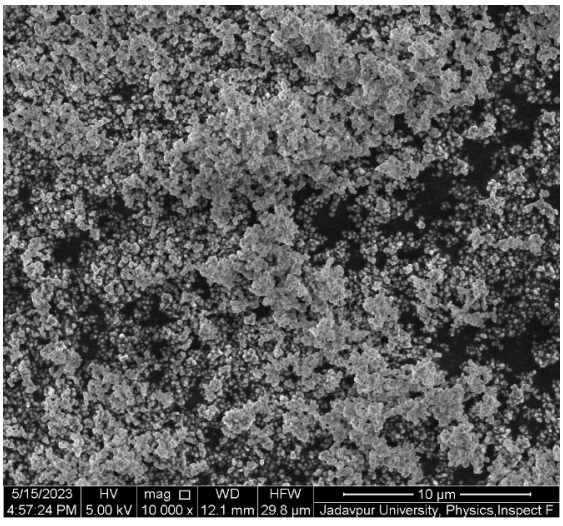


(a)

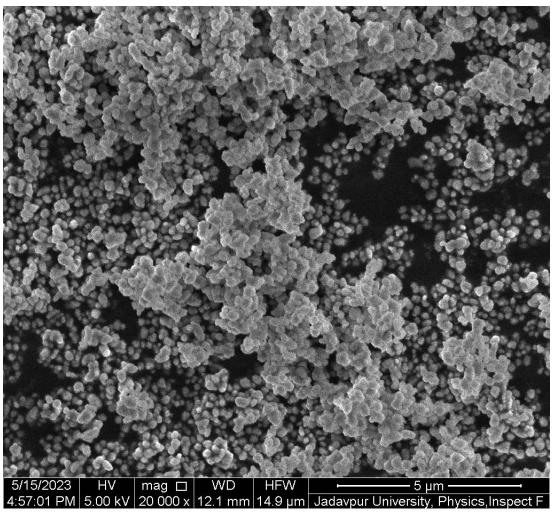


(b)

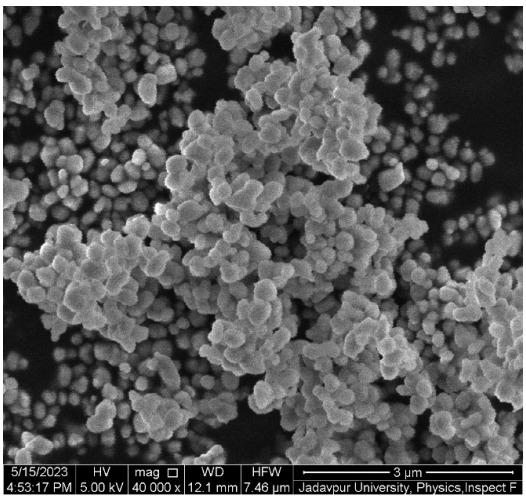


(c)

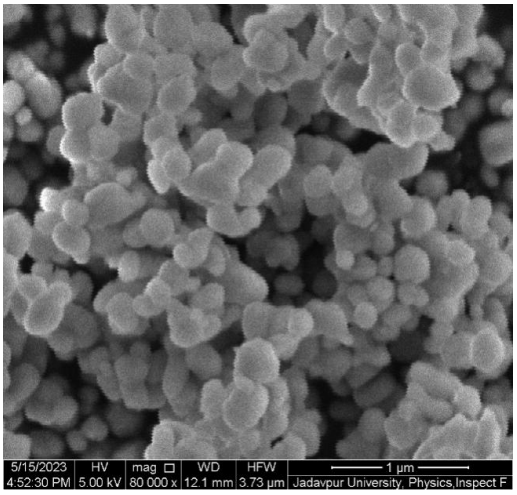


(d)

Figure 5.7 SEM image at different ranges (a) 10 um (b) 5 um (c) 3 um (d) 1 um

## 5.3.2 Carbon Particles

SEM analysis of carbon particles displays a diverse range of morphologies. Figures 5.8 (a), 5.8 (b), 5.8 (c) ,and 5.8 (d) depict the presence of both irregularly shaped and elongated carbon particles. The irregular carbon particles exhibit rough surfaces, suggesting a high degree of surface complexity. The elongated carbon particles display lengths ranging from 500 nm to 20 µm, with varying aspect ratios.

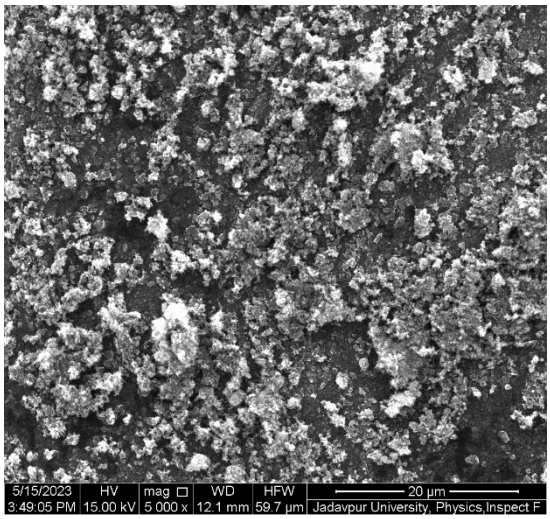


(a)

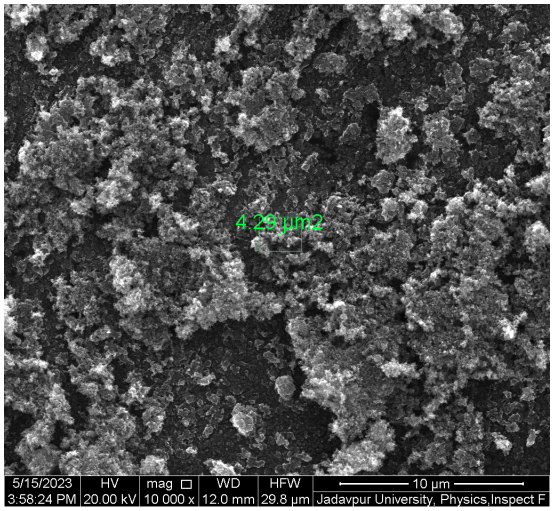


(b)

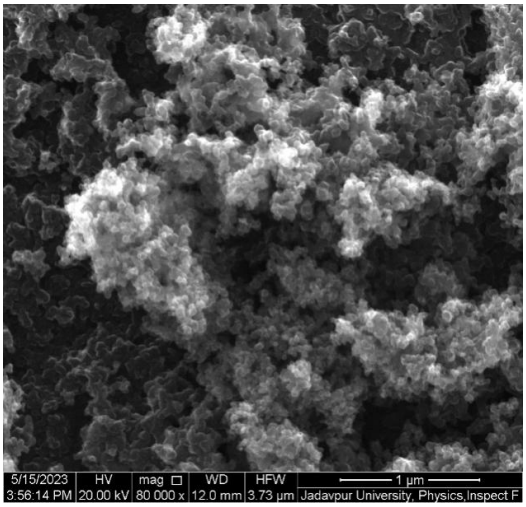


(c)

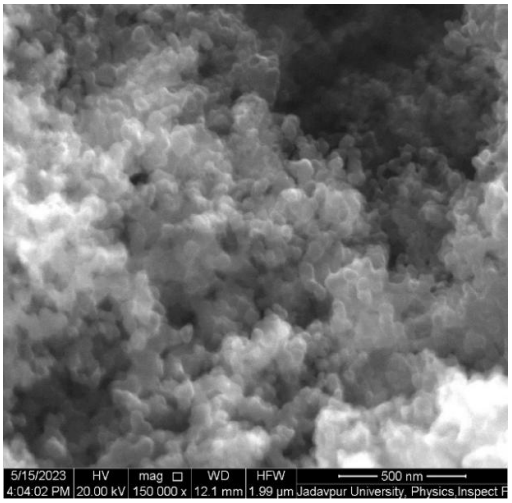


(d)

Figure 5.8 SEM Image at different ranges (a) 20 um (b) 10 um (c) 1 um (d) 500 nm

The obtained SEM images and quantitative data allow for a comprehensive understanding of the particle morphologies, enabling the tailoring of materials for specific applications. The SEM analysis reveals the distinct morphological characteristics of $TiO_2$ and carbon particles. The well-defined spherical shape and uniform size distribution of $TiO_2$ particles make them suitable for various applications requiring controlled particle properties. The diverse morphologies of carbon particles, including irregular shapes and elongated structures, offer versatility for different functional applications. These findings contribute to the understanding of particle morphology and aid in the design and optimization of materials for specific purposes.

## 5.4 X-Ray Diffraction (XRD) Analysis

XRD analysis provides valuable information regarding the crystallographic structure and phase composition of the DSSC components. By analyzing the diffraction patterns, we can determine the degree of crystallinity and identify the presence of any impurities or undesirable phases that could hinder the efficiency of the solar cell. This analysis aids in understanding the structural stability and integrity of the DSSC materials. The XRD pattern of the $TiO_2$ particles is shown in Figure-5.9. The diffraction peaks are observed at 2θ angles of 27.3°, 35.9°, 41.0°, 54.0°, and 68.6°corresponds to the (110), (101), (111), (211), (211), and (301) crystallographic planes, respectively. This confirms the crystalline nature of the $TiO_2$ particles. This confirms the crystalline nature of the $TiO_2$ particles.

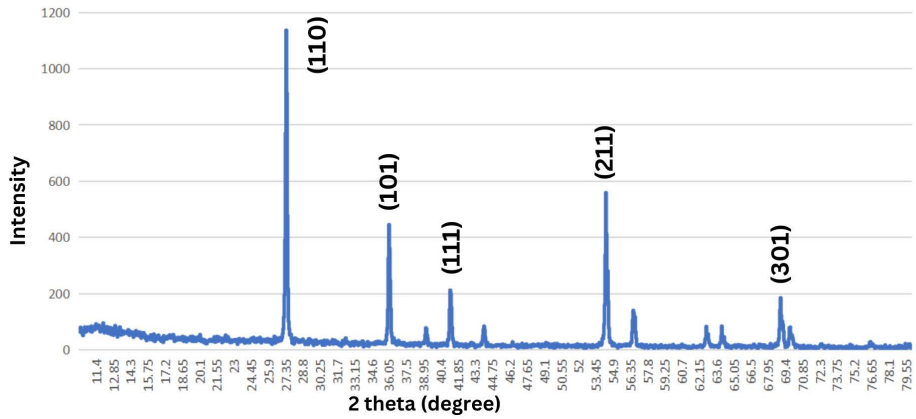


Figure 5.9 XRD Pattern

The XRD analysis of the $TiO_2$ particles confirms the presence of the rutile phase with a crystallinity. The absence of impurity peaks suggests the high purity of the particles. The obtained XRD results are consistent with the expected crystal structure of $TiO_2$, validating its suitability for various applications such as photocatalysis, solar cells, and sensors.

# 5.5 Spectrophotometry Analysis

Spectrophotometry analysis offers insights into the optical properties of the alternative dyes used in the DSSCs. By measuring the absorption spectra, we can evaluate the dye's light-harvesting efficiency and the wavelength range in which it exhibits maximum absorption. This information helps in selecting dyes that effectively capture a broad spectrum of light and convert it into electrical energy. Spectrophotometric Analysis of Methyl Violet Synthetic Dye, Prussian Blue Acrylic Color-dye, and Bougainvillea Extract as Agro-waste Sample using UV-Vis Spectrophotometer Lambda 25

## 5.5.1 Methyl Violet Dye

Absorbance Spectra: The UV-Vis spectrum of methyl violet synthetic dye showed a characteristic approximately peak at $\lambda_{max}$ = 580 nm as shown in the Figure-5.10, indicating the absorption of light in the visible range.

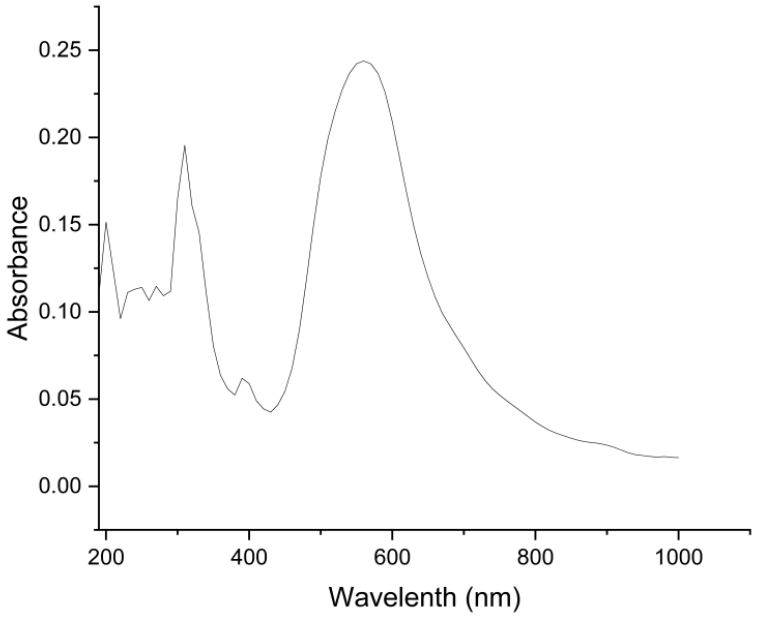


Figure 5.10 UV-Visible Absorption Spectra of Methyl Violet Dye

## 5.5.2 Prussian Blue Acrylic Color-dye

Absorbance Spectra: The UV-Vis spectrum of Prussian blue acrylic dye exhibited absorption approximately peaks at $\lambda_{max}$ = 300 nm, 650 nm, and 710 nm, Figure-5.11 suggesting absorption in the UV region, a little bit in the visible region, and also in the near-infrared region.

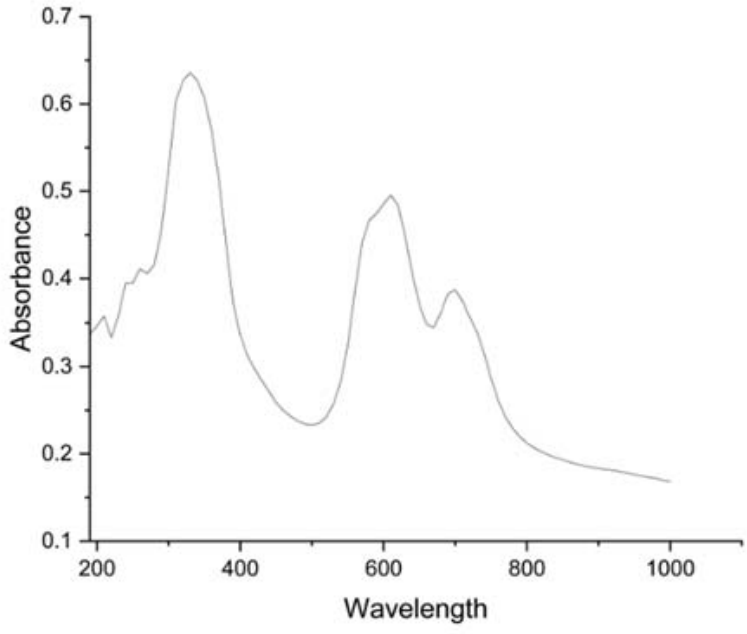


Figure5.11 UV-Visible Absorption Spectra of Prussian Blue Acrylic Color

## 5.5.3 Bougainvillea Extract as Agro-waste Dye

Absorbance Spectra: The UV-Vis spectrum of bougainvillea extract displayed characteristic absorption approximately peaks at λmax = 380 nm, various wavelengths, indicating the absorption of light in the starting range of visible region as shown in figure 5.12

The results obtained from the spectrophotometric analysis of the three samples provided valuable insights into their absorbance spectra and concentration levels. Methyl violet synthetic dye exhibited a distinct absorption peak in the visible region, indicating its suitability for coloring applications. Prussian blue acrylic color, on the other hand, demonstrated absorption peaks at various wavelengths. The bougainvillea extract obtained showed absorption peaks at the beginning of the visible region, suggesting the presence of various compounds with different absorption characteristics.

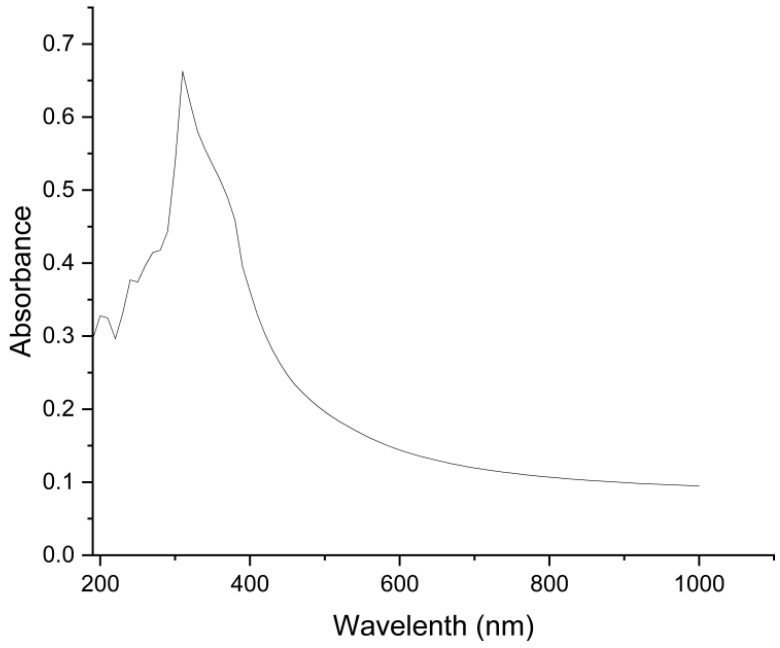


Figure 5.12 UV-Visible Absorption Spectra of Agro-waste dye

Overall, the spectrophotometric analysis using the UV-Vis Spectrophotometer Lambda 25 proved to be an effective method for the determination of concentrations and absorbance spectra of Methyl violet synthetic dye, Prussian blue acrylic color-dye, and Bougainvillaea dye treated as agro-waste based dye. These findings contribute to a better understanding of the properties and potential applications of these samples in various industries.

# 5.6 J-V Characteristics

The J-V (current-voltage) curve analysis was conducted to evaluate the performance of three different dyes: methyl violet, Prussian blue acrylic colour-dye, and an agro-waste dye. To measure the current and voltage, a variable resistor circuit was set up and connected to a data logger (as shown in the schematic diagram Figure 5.4 ), which acted as a voltmeter and ammeter for all those samples, allowing for real-time data collection under natural sunlight conditions. In the city of Kolkata, where the experiment is conducted, the solar intensity typically ranges from 400 to 600 W/m$^2$. Therefore, we have collected data under conditions of moderate intensity, specifically ranging from approximately 380 to 420 W/m$^2$. The solar intensity is measured by a Solar Power meter (Figure-4.6). The purpose of observing the performance of DSSCs under this moderate natural intensity is to study their behavior under realistic and representative conditions. The J-V curve analysis provides insights into the electrical behavior of the dye-sensitized solar cells (DSSCs) and helps assess their efficiency. In this study, it was observed that the DSSCs based on the natural agro-waste dye exhibited superior performance compared to the other two dyes. The J-V curve represents the relationship between the current density (J) and the voltage (V) across the solar cell. It characterizes the device's ability to convert sunlight into electrical energy. By varying the load resistance, different data points were obtained, and the J-V curve was plotted.

# 5.7 J-V Curve of DSSCs

# 5.7.1 Methyl Violet Synthetic dye based DSSC

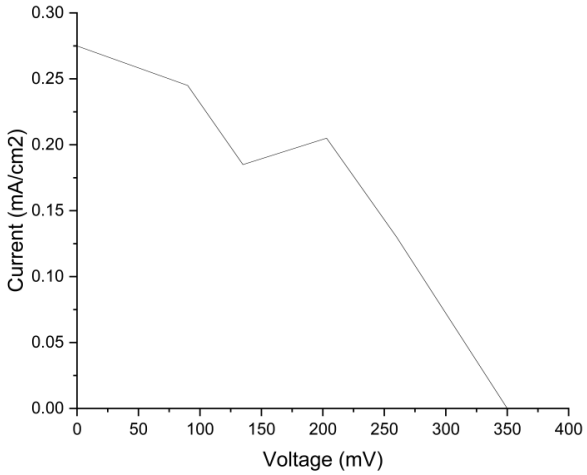


Figure 5.13 J-V Characteristics of Methyl Violet Synthetic dye

The J-V (current-voltage) analysis of a Methyl Violet Synthetic dye-based DSSC under the natural solar intensity of 405 W/m$^2$ (Figure 5.13) is summarized as follows:
Under applied load resistance, the Methyl Violet Synthetic dye-based DSSC generated a maximum current (Jmp) of 0.28 mA/cm$^2$ and a maximum voltage of 366 mV.

The fill factor (FF) is a measure of how well the DSSC utilizes the available voltage and current. It is calculated by taking the ratio of the maximum power point (Pmax) to the product of Jsc and voc. The calculated FF is 0.44, indicating the efficiency of power conversion within the DSSC.

Efficiency is a crucial parameter that indicates the overall performance of the DSSC. It is calculated by taking the ratio of the maximum power output to the incident solar power of 405 W/m2. In this case, the efficiency is 0.25%.

## 5.7.2 Prussian Blue Acrylic color-dye based DSSC

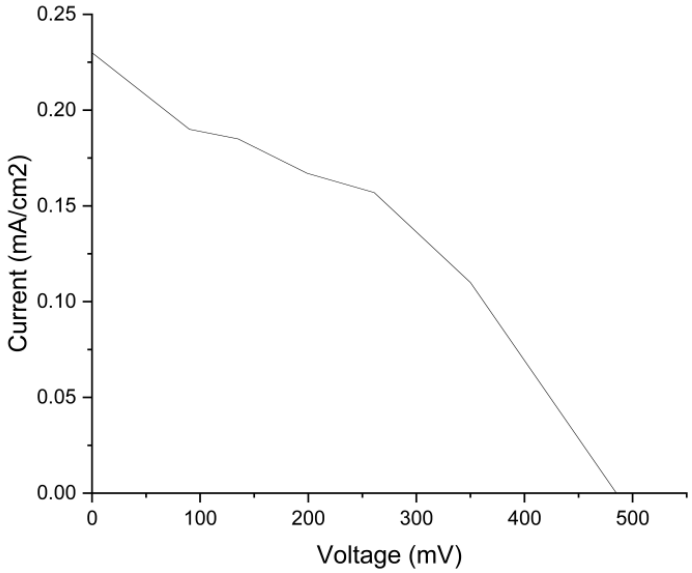


Figure 5.14 J-V Characteristic of Prussian Blue Acrylic color

The J-V analysis of a DSSC utilizing a Prussian Blue acrylic color-dye, operating under the natural solar intensity of 410 W/m$^2$ (Figure-5.14) is summarized as follows: At a specific applied load resistance, the DSSC employing a Methyl Violet Synthetic dye achieved a maximum current (Jmp) of 0.22 mA/cm$^2$ and a maximum voltage of 294 mV.

The fill factor (FF) serves as an indicator of how effectively the DSSC utilizes the available voltage and current. It can be determined by dividing the maximum power point (Pmax) by the product of Jsc and Voc. The calculated FF is 0.36, which suggests the efficiency of power conversion within the DSSC.

Efficiency, a crucial parameter for assessing the overall performance of the DSSC, can be computed by dividing the maximum power output by the incident solar power of 405 W/m2. In this case, the efficiency amounts to 0.24%.

## 5.7.3 Agro-waste dye-based DSSC

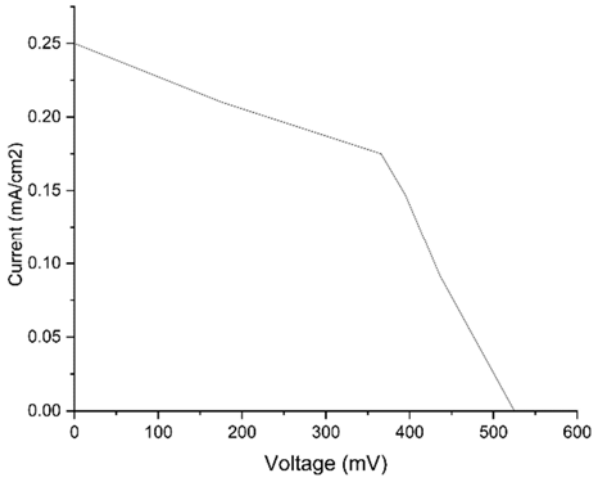


Figure 5.15 J-V Characteristic of Agro-waste dye-based DSSC

The J-V (current-voltage) (Figure-5.15) analysis of an Agro-waste dye-based Dye-Sensitized Solar Cell (DSSC) under a solar intensity of 395 W/m$^2$. This particular DSSC generated a maximum current of 0.27 mA/cm$^2$ with a load resistance under specified natural sunlight.

The fill factor (FF) is a measure of how effectively the DSSC utilizes the available power. A fill factor of 0.48 indicates that the DSSC can convert 48% of the maximum available power into usable electrical power.

The efficiency of the DSSC is calculated as the ratio of the maximum power output to the incident solar power. The calculated efficiency is 0.39%, which means that the DSSC converts 0.39% of the incident solar power into usable electrical power.

## 5.8 Fill Factor Analysis

The fill factor (value shown in the Table-5.1 ) is a measure of how effectively a solar cell can convert incident light into electrical power. It is determined by factors such as charge transport, recombination, and resistive losses within the device. The product of Impp (maximum current) and Vmpp (maximum voltage) that yields the highest power delivered to the load is smaller than the product of the largest current that can be extracted from the cell (Isc) multiplied by the higher voltage (Voc). The fill factor (FF) is defined as the quotient of Impp multiplied by Vmpp divided by Isc multiplied by Voc. The fill factor is always less than unity and is commonly used as a measure of the shape of the characteristic curve. The form factor is a practical parameter with significant utility.

The fill factor is calculated using the following formula:

$$FF = \frac{Vmp * Imp}{Voc * Isc}$$

For DSSCs, we must consider the active area of the solar cell (A).

$$Short\ Circuit\ Current\ Density\ (Jsc) = \frac{Isc}{A}$$

$$Maximum\ Current\ Density\ (Jmp) = \frac{Imp}{A}$$

The fill factor for DSSCs is calculated using the following formula:

$$FF = \frac{Vmp * Jmp}{Voc * Jsc}$$

From this the maximum power delivered by the DSSC:

$$Pmax = FF * Voc * Jsc$$

## 5.9 Efficiency Analysis

The efficiency of a solar cell is a key parameter that determines its ability to convert sunlight into electrical power. It is calculated by dividing the maximum power output of the solar cell by the incident power of the light source.

The efficiency (η) can be expressed as:

$$Efficiency\ (\eta\%) = \frac{Vmp * Jmp * 100}{Pin * A}$$

Pin- Incident Radiation Flux ($W/m^2$)
Here the active area of the cell - length- 0.8 cm and width- 0.8 cm,
the active area of cell- $0.64cm^2$

Table 5.1 Electrical Parameters of different dyes

| Dye | Intensity (Pin) W/m2 | Voc (mV) | Jsc ($mA/cm^2$) | FF | Efficiency |
|---|---|---|---|---|---|
| Agro-waste Dye | 395 | 525 | 0.390 | 0.48 | 0.39 |
| Methyl Violet | 405 | 405 | 0.429 | 0.44 | 0.25 |
| Acrylic Colour-dye | 410 | 410 | 0.359 | 0.36 | 0.24 |

The analysis revealed that the DSSCs utilizing the methyl violet dye demonstrated higher short-circuit current density (Jsc), but Agro-waste dye performed best in terms of FF and efficiency values compared to the DSSCs employing methyl violet and Prussian blue acrylic color dye as shown in Table 5.1. These parameters are critical for determining the overall performance and efficiency of the solar cell.

The efficient performance of the DSSCs based on the natural agro-waste dye can be attributed to several factors. Agro-waste dyes often contain a variety of natural pigments and organic compounds that can effectively absorb sunlight across the visible spectrum.

## 5.10 Conclusion

The efficient performance of the DSSCs based on the natural agro-waste dye can be attributed to several factors. Agro-waste dyes often contain a variety of natural pigments and organic compounds that can effectively absorb sunlight across the UV-Visible spectrum.

In conclusion, the use of SEM, XRD, spectrophotometry, and J-V characteristics analysis in the investigation of DSSCs (dye-sensitized solar cells) has provided valuable insights into their performance and potential applications.

The utilization of various characterization techniques has facilitated a thorough analysis of the dye-sensitized solar cells (DSSCs) under investigation, leading to the generation of significant results. The interpretation and discussion of these results have provided valuable insights into the performance, efficiency, and potential improvements of DSSCs. By drawing upon the findings discussed, this study concludes with key recommendations and implications for future research scopes in the field of DSSCs.

# Chapter-6
# Conclusion

## 6.1 Conclusion

In this thesis, entirely the design of DSSCs, fabrication process with various dyes and the their analysis are discussed. The performance of the dye extracted from bougainvillea was compared to methyl violet dye and Prussian blue acrylic color dye. The results revealed that the dye extracted from bougainvillea outperformed compared with the other dyes in terms of its effectiveness as a sensitizer for DSSCs. Furthermore, the dye was preserved for 30 days and it came up with the efficiency of 0.39% and fill factor of 0.48. This finding indicates the potential for long-term utilization of agro-waste-based dyes in DSSCs. By effectively preserving the dye, it can be used for extended periods, making it a sustainable and cost-effective option for solar cell applications. Meanwhile, the methyl violet based DSSC generated the highest current density of 0.429 mA/cm$^2$.

The results obtained in this study, demonstrate the potential of Prussian Blue Acrylic Colour-Dye as a new type of sensitizer in the field of DSSCs with efficiency of 0.24%. Prussian Blue, traditionally used in the textile industry, has opened new doors of opportunity for its application in DSSCs. Its superior performance in this study suggests that it can be a promising alternative to conventional sensitizers in solar cell technology.
In conclusion, the first chapter introduces energy scenarios, justifies Dye-Sensitized Solar Cell (DSSC) research, and addresses energy challenges. Then chapter 2 is all about the literature survey of previous work, emphasizing dyes and fabrication processes.

Chapter 3 explains entire theory of DSSC with structure and operation, covering electron transfer, charge transport, and light absorption. Chapter 4 details the effective experimental setup and methodology for fabrication. At the end of the experiment, Chapter 5 presents experimental results, that helps to compare and analysis between different dyes.

The entirety of this research work draws inspiration from a range of previous research studies, each of which leads original technological advancements. Through a thorough comparative analysis, the results demonstrate a high level of satisfaction and perform admirably when compared to other research endeavors. These findings, when coupled with appropriate techniques, hold considerable value for researchers as they undertake further investigations as an outcome of this thesis. The subsequent section of this chapter explores several future prospects that can be pursued based on the outcomes of this study.

## 6.2 Future Scope

The research conducted in this thesis lays the foundation for future studies and advancements in the field of DSSCs. The following are some potential areas of future research and development:

### 6.2.1 Agro-waste Preservation

The concept of utilizing agricultural waste-based dyes for solar cell applications can be further pursued. This research demonstrates the potential of extracting dyes from agricultural waste, which not only provides a sustainable and environmentally friendly approach but also presents economic benefits by utilizing waste materials. By exploring different agro-waste sources and optimizing the extraction process, a wide range of potential dyes can be identified, enhancing the scope of sustainable and cost-effective DSSCs.

### 6.2.2 Optimization of Prussian Blue Acrylic Colour-Dye

Further investigations can be carried out to optimize the fabrication process and parameters of DSSCs using Prussian Blue Acrylic Colour Dye. This includes exploring different concentrations, thicknesses, and methods of dye application to enhance the efficiency and stability of the solar cells.

### 6.2.3 Performance under different natural intensities

The performance of these DSSCs can be observed and studied under different natural intensities of sunlight. This would help in understanding how solar cells respond to varying light conditions and their adaptability in real-world applications.

### 6.2.4 Stability and durability studies

The long-term stability and durability of these three dye-based DSSCs need to be investigated to assess their performance over an extended period. This includes examining

the effects of temperature, humidity, and aging on the efficiency and functionality of solar cells.

### 6.2.5 Scale-up and commercialization

Efforts should be made to scale up the production of Agro-waste dye and Prussian Blue Acrylic Colour-dye based DSSCs and explore their commercial viability. This involves optimizing the fabrication process for mass production and assessing the cost-effectiveness of the solar cells.

### 6.2.6 Integration with the textile industry

The potential integration of Prussian Blue Acrylic Color Dye-based DSSCs with the textile industry should be explored. This includes developing solar cell-integrated textiles and wearable devices that can generate electricity from sunlight.

# References


1. Energy Production and Consumption - Our World in Data
2. India Energy Outlook 2021 – Analysis - IEA
3. Ministry of Coal, Government of India
4. INFOGRAPHIC: Installed capacity versus gross power generation in India, ET EnergyWorld (indiatimes.com)
5. Global EV Outlook 2021 – Analysis - IEA
6. Bansal, Mohit, R. P. Saini, and Dheeraj Kumar Khatod. "Development of cooking sector in rural areas in India—A review." *Renewable and Sustainable Energy Reviews* 17 (2013): 44-53.
7. India needs more investments to meet renewables target - India Climate Dialogue
8. india: India to achieve 50% clean energy share, 500 GW RE capacity targets before 2030 deadline: RK Singh - The Economic Times (indiatimes.com)
9. India's-Energy-Efficiency-Landscape-Report.pdf (aeee.in)
10. pib.gov.in/PressReleaseIframePage.aspx?PRID=1717977
11. Jawaharlal Nehru National Solar Mission (Phase I, II and III) – Policies - IEA
12. UJALA (Unnat Jyoti by Affordable LEDs for All) Scheme | IBEF
13. Aggarwal, Shubham, Sudhanshu Kumar, and Manoj Kumar Tiwari. "Decision support system for Pradhan Mantri Ujjwala Yojana." *Energy Policy* 118 (2018): 455-461.
14. BEE_ECBC 2017.pdf (beeindia.gov.in)
15. World Energy Outlook 2021 (windows.net)
16. Where does our power sector stand? | Electrical India Magazine
17. India to overtake China as world's most populous country in April 2023, United Nations projects | United Nations
18. Singh, Manoj Kumar, Sadhan Mahapatra, and S. K. Atreya. "Green building design: A step towards sustainable habitat." In *Natl Conf Renewable Energy*, vol. 2010, no. NCRE2010, pp. 257-268. 2010.
19. Industrial Demand and Energy Supply Management | CEEW
20. Pinna, I., B. Dalla Chiara, and K. Pant. "Energy used by transport systems in India: The role of the urban population, sources, alternative modes and quantitative analyses." *WIT Transactions on Ecology and the Environment* 190 (2014): 661-675.

21. Web copy of AR (Eng)_7.pdf (agricoop.nic.in)
22. India becomes power surplus nation with electricity capacity of over four lakh Mega Watt (newsonair.gov.in)
23. Press Information Bureau (pib.gov.in)
24. http://www.nrel.gov/rredc/solar_data.html; © 2019 The World Bank, Source: Global Solar Atlas 2.0, Solar resource data: Solargis
25. Kumar, C. R., and M. A. Majid. "Renewable energy for sustainable development in India: Current status, future prospects, challenges, employment, and investment opportunities." *TIDEE: TERI Information Digest on Energy and Environment* 21, no. 1 (2022): 33-33.
26. India Energy Outlook 2021
27. Current Status | Ministry of New and Renewable Energy, Government of India (mnre.gov.in)
28. Schlömer, Steffen, Thomas Bruckner, Lew Fulton, Edgar Hertwich, Alan McKinnon, Daniel Perczyk, Joyashree Roy et al. "Annex III: Technology-specific cost and performance parameters." In *Climate change 2014: Mitigation of climate change: Contribution of working group III to the fifth assessment report of the Intergovernmental Panel on Climate Change*, pp. 1329-1356. Cambridge University Press, 2014.
29. India can achieve 30% of renewable energy by 2030: TERI - GreentechLead
30. Home - BRIDGE TO INDIA
31. Hagfeldt, Anders, Gerrit Boschloo, Licheng Sun, Lars Kloo, and Henrik Pettersson. "Dye-sensitized solar cells." *Chemical reviews* 110, no. 11 (2010): 6595-6663.
32. Pecunia, Vincenzo, Luigi G. Occhipinti, and Robert LZ Hoye. "Emerging indoor photovoltaic technologies for sustainable internet of things." *Advanced Energy Materials* 11, no. 29 (2021): 2100698.
33. Photovoltaic Effect - an overview | ScienceDirect Topics
34. Photovoltaics: A History Of Our Cleanest Energy - The Institution for Science Advancement (ifsa.my)
35. Williams, Richard. "Becquerel photovoltaic effect in binary compounds." *The journal of Chemical physics* 32, no. 5 (1960): 1505-1514.
36. Gerischer, H., M. E. Michel-Beyerle, F. Rebentrost, and H. Tributsch. "Sensitization of charge injection into semiconductors with large band gap." *Electrochimica Acta* 13, no. 6 (1968): 1509-1515.

37. Tributsch, Helmut, and Melvin Calvin. "Electrochemistry of excited molecules: photo-electrochemical reactions of chlorophylls." *Photochemistry and Photobiology* 14, no. 2 (1971): 95-112.
38. Matsumura, Michio, Shigeyuki Matsudaira, Hiroshi Tsubomura, Masasuke Takata, and Hiroaki Yanagida. "Dye sensitization and surface structures of semiconductor electrodes." *Industrial & Engineering Chemistry Product Research and Development* 19, no. 3 (1980): 415-421.
39. O'regan, Brian, and Michael Grätzel. "A low-cost, high-efficiency solar cell based on dye-sensitized colloidal TiO2 films." *nature* 353, no. 6346 (1991): 737-740.
40. https://www.sciencedirect.com/science/article/pii/S1369702114003216
41. Han, Deok-Woo, Jong-Hyun Heo, Dong-Joo Kwak, Chi-Hwan Han, and Youl-Moon Sung. "Texture, Morphology and Photovoltaic Characteristics of Nanoporous F: $SnO_2$ Films." *Journal of Electrical Engineering & Technology* 4, no. 1 (2009): 93-97.
42. Jeng, Ming-Jer, Yi-Lun Wung, Liann-Be Chang, and Lee Chow. "Particle size effects of TiO2 layers on the solar efficiency of dye-sensitized solar cells." *International Journal of Photoenergy* 2013 (2013).
43. Wang, Wei, Huihui Yuan, Junjie Xie, Di Xu, Xinyu Chen, Yunlong He, Tao Zhang, Zongqi Chen, Yumei Zhang, and Hujiang Shen. "Enhanced efficiency of large-area dye-sensitized solar cells by light-scattering effect using multilayer TiO2 photoanodes." *Materials Research Bulletin* 100 (2018): 434-439.
44. Wang, Zhong-Sheng, Masatoshi Yanagida, Kazuhiro Sayama, and Hideki Sugihara. "Electronic-insulating coating of CaCO3 on TiO2 electrode in dye-sensitized solar cells: improvement of electron lifetime and efficiency." *Chemistry of Materials* 18, no. 12 (2006): 2912-2916.
45. Arunmetha, S., V. Rajendran, M. Vinoth, A. Karthik, S. R. Srither, M. Srither Panday, N. Nithyavathy, P. Manivasakan, and M. Maaza. "An efficient photoanode for dye sensitized solar cells using naturally derived S/TiO2 nanoparticles." *Materials Research Express* 4, no. 3 (2017): 035016.
46. Agrawal, Anupam, Shahbaz A. Siddiqui, Amit Soni, Kanupriya Khandelwal, and Ganesh D. Sharma. "Performance analysis of TiO2 based dye sensitized solar cell prepared by screen printing and doctor blade deposition techniques." *Solar Energy* 226 (2021): 9-19.

47. Subramanian, Alagesan, and Hong-Wen Wang. "Hierarchical multilayer-structured TiO2 electrode for dye-sensitized solar cells." *Journal of Photochemistry and Photobiology A: Chemistry* 279 (2014): 32-37.
48. Rajaramanan, Tharmakularasa, Fatemeh Heidari Gourji, Dhayalan Velauthapillai, Punniamoorthy Ravirajan, and Meena Senthilnanthanan. "Enhanced Photovoltaic Properties of Dye-Sensitized Solar Cells through Ammonium Hydroxide-Modified (Nitrogen-Doped) Titania Photoanodes." *International Journal of Energy Research* 2023 (2023).
49. Naik, Praveen, Islam M. Abdellah, M. Abdel-Shakour, Rui Su, Kavya S. Keremane, Ahmed El-Shafei, and Airody Vasudeva Adhikari. "Improvement in performance of N3 sensitized DSSCs with structurally simple aniline based organic co-sensitizers." *Solar Energy* 174 (2018): 999-1007.
50. Subramaniam, Kamalesu, Anish Babu Athanas, and Swarnalatha Kalaiyar. "Dual anchored Ruthenium (II) sensitizer containing 4-Nitro-phenylenediamine Schiff base ligand for dye sensitized solar cell application." *Inorganic Chemistry Communications* 104 (2019): 88-92.
51. Cong, Jiayan, Xichuan Yang, Jing Liu, Jinxia Zhao, Yan Hao, Yu Wang, and Licheng Sun. "Nitro group as a new anchoring group for organic dyes in dye-sensitized solar cells." *Chemical Communications* 48, no. 53 (2012): 6663-6665.
52. Hao, Yan, Yasemin Saygili, Jiayan Cong, Anna Eriksson, Wenxing Yang, Jinbao Zhang, Enrico Polanski et al. "Novel blue organic dye for dye-sensitized solar cells achieving high efficiency in cobalt-based electrolytes and by co-sensitization." *ACS applied materials & interfaces* 8, no. 48 (2016): 32797-32804.
53. Sharma, Govind, Vidyadhar Singh, S. N. Dolia, I. P. Jain, Pankaj K. Jain, and Chhagan Lal. "Present status of metal-free photosensitizers for dye-sensitized solar cells." *Materials Today: Proceedings* (2023).
54. Yang, Liu, Zhiwei Zheng, Yan Li, Wenjun Wu, He Tian, and Zhaohui Wang. "N-Annulated perylene-based metal-free organic sensitizers for dye-sensitized solar cells." *Chemical communications* 51, no. 23 (2015): 4842-4845.
55. Naik, Praveen, Rui Su, Mohamed R. Elmorsy, Ahmed El-Shafei, and Airody Vasudeva Adhikari. "Investigation of new carbazole based metal-free dyes as active photo-sensitizers/co-sensitizers for DSSCs." *Dyes and Pigments* 149 (2018): 177-187.

56. Narayanaswamy, K., T. Swetha, Gaurav Kapil, Shyam S. Pandey, Shuzi Hayase, and Surya Prakash Singh. "Simple metal-free dyes derived from triphenylamine for DSSC: A comparative study of two different anchoring group." *Electrochimica Acta* 169 (2015): 256-263.
57. Feng, Haijing, Ranran Li, Yicong Song, Xiaoyan Li, and Bo Liu. "Novel D-π-A-π-A coumarin dyes for highly efficient dye-sensitized solar cells: Effect of π-bridge on optical, electrochemical, and photovoltaic performance." *Journal of Power Sources* 345 (2017): 59-66.
58. Ammar, Ahmed M., Hemdan SH Mohamed, Moataz MK Yousef, Ghada M. Abdel-Hafez, Ahmed S. Hassanien, and Ahmed SG Khalil. "Dye-sensitized solar cells (DSSCs) based on extracted natural dyes." *Journal of Nanomaterials* 2019 (2019).
59. Abdel-Latif, Monzir S., Mahmoud B. Abuiriban, Taher M. El-Agez, and Sofyan A. Taya. "Dye-sensitized solar cells using dyes extracted from flowers, leaves, parks, and roots of three trees." *International Journal of Renewable Energy Research* 5, no. 1 (2015): 294-298.
60. Kabir, Fahmid, Md Mosharraf Hossain Bhuiyan, Md Robiul Hossain, Md Serajum Manir, Md Saifur Rahaman, M. Tauhidul Islam, and Saeed Mahmud Ullah. "Refining of red spinach extract for the enhanced photovoltaic performance of natural dye-based DSSC and degradation study." *Optik* 251 (2022): 168452.
61. Setiawan, I. Nyoman, I. D. Giriantari, W. Ariastina, and I. A. Swamardika. "Natural dyes extracted from bioactive components of fruit waste for dye-sensitized solar cell." *India: International Research Publication House* (2020).
62. El-Agez, Taher M., Sofyan A. Taya, Kamal S. Elrefi, and Monzir S. Abdel-Latif. "Dye-sensitized solar cells using some organic dyes as photosensitizers." *Optica applicata* 44, no. 2 (2014): 345-351.
63. Muzakkar, M. Z., D. Wibowo, and M. Nurdin. "A novel of buton asphalt and methylene blue as dye-sensitized solar cell using TiO2/Ti nanotubes electrode." In *IOP Conference Series: Materials Science and Engineering*, vol. 267, no. 1, p. 012035. IOP Publishing, 2017.
64. Ranamagar, Bandana, Isaac Abiye, and Fasil Abebe. "Dye-sensitized solar cells on TiO2 Photoelectrodes sensitized with rhodamine." *Materials Letters* (2023): 133887.
65. Richhariya, Geetam, and Anil Kumar. "Fabrication and characterization of mixed dye: Natural and synthetic organic dye." *Optical Materials* 79 (2018): 296-301.

66. Nakhaei, Roohollah, Alireza Razeghizadeh, Pejman Shabani, Jabbar Ganji, and Seyed Sajjad Tabatabaee. "Photoabsorption Enhancement in Synthetic-Natural Dye-Sensitized Solar Cells Using Bilayer TiO2 Deposition and Separated Sensitization." *International Journal of Photoenergy* 2022 (2022).
67. Richhariya, Geetam, Anil Kumar, Akash Kumar Shukla, Kailash Nath Shukla, and Issara Chanakaewsomboon. "Efficient photosensitive light harvesting dye sensitized solar cell using hibiscus and rhodamine dyes." *Journal of Power Sources* 572 (2023): 233112.
68. Ji, Jung-Min, Haoran Zhou, Yu Kyung Eom, Chul Hoon Kim, and Hwan Kyu Kim. "14.2% efficiency dye-sensitized solar cells by co-sensitizing novel thieno [3, 2-b] indole-based organic dyes with a promising porphyrin sensitizer." *Advanced Energy Materials* 10, no. 15 (2020): 2000124.
69. Wante, Haruna P., Joseph Aidan, and Sabastine C. Ezike. "Efficient dye-sensitized solar cells (DSSCs) through atmospheric pressure plasma treatment of photoanode surface." *Current Research in Green and Sustainable Chemistry* 4 (2021): 100218.
70. Azmar, Amisha, R. H. Y. Subban, and Tan Winie. "Improved long-term stability of dye-sensitized solar cell employing PMA/PVAc based gel polymer electrolyte." *Optical Materials* 96 (2019): 109349.
71. Chalkias, D. A., N. E. Verykokkos, E. Kollia, A. Petala, V. Kostopoulos, and G. C. Papanicolaou. "High-efficiency quasi-solid state dye-sensitized solar cells using a polymer blend electrolyte with “polymer-in-salt” conduction characteristics." *Solar Energy* 222 (2021): 35-47.
72. Wang, Dafu, Wei Wei, and Yun Hang Hu. "Highly efficient dye-sensitized solar cells with composited food dyes." *Industrial & Engineering Chemistry Research* 59, no. 22 (2020): 10457-10463.
73. Althagafi, Ismail, and Nashwa El-Metwaly. "Enhancement of dye-sensitized solar cell efficiency through co-sensitization of thiophene-based organic compounds and metal-based N-719." *Arabian Journal of Chemistry* 14, no. 4 (2021): 103080.

74. H. Ritchie, Energy Mix, https://ourworldindata.org/energy-mix.
75. D. Archer, Global Warming: Understanding the Forecast, John Wiley & Sons, 2nd edn, 2012 Search PubMed .
76. H. Ritchie and M. Roser, Renewable Energy, https://ourworldindata.org/renewable-energy.

77. IEA, Renewables 2020, International Energy Agency, 2020 DOI:10.1787/c74616c1-en.
78. B. O'Regan and M. Grätzel, Nature, 1991, 353, 737–740 CrossRef .
79. H. Gerischer, J. Electrochem. Soc., 1966, 113, 1174 CrossRef CAS .
80. H. Gerischer, Electrochim. Acta, 1990, 35, 1677–1699 CrossRef CAS .
81. A. Hagfeldt, G. Boschloo, L. Sun, L. Kloo and H. Pettersson, Chem. Rev., 2010, 110, 6595–6663 CrossRef CAS PubMed .
82. M. Stojanović, N. Flores-Diaz, Y. Ren, N. Vlachopoulos, L. Pfeifer, Z. Shen, Y. Liu, S. M. Zakeeruddin, J. V. Milić and A. Hagfeldt, Helv. Chim. Acta, 2021, 104, e2000230 CrossRef .
83. I. Benesperi, H. Michaels and M. Freitag, J. Mater. Chem. C, 2018, 6, 11903–11942 RSC .
84. M. Freitag and G. Boschloo, Curr. Opin. Electrochem., 2017, 2, 111–119 CrossRef CAS.
85. D. Zhang, M. Stojanovic, Y. Ren, Y. Cao, F. T. Eickemeyer, E. Socie, N. Vlachopoulos, J.-E. Moser, S. M. Zakeeruddin, A. Hagfeldt and M. Grätzel, Nat. Commun., 2021, 12, 1777 CrossRef CAS PubMed .
86. M. Grätzel, J. Photochem. Photobiol., C, 2003, 4, 145–153 CrossRef .
87. Y. Saygili, M. Söderberg, N. Pellet, F. Giordano, Y. Cao, A. B. Muñoz-García, S. M. Zakeeruddin, N. Vlachopoulos, M. Pavone, G. Boschloo, L. Kavan, J.-E. Moser, M. Grätzel, A. Hagfeldt and M. Freitag, J. Am. Chem. Soc., 2016, 138, 15087–15096 CrossRef CAS PubMed .
88. R. Harikisun and H. Desilvestro, Sol. Energy, 2011, 85, 1179–1188 CrossRef CAS .
89. A. Hinsch, J. M. Kroon, R. Kern, I. Uhlendorf, J. Holzbock, A. Meyer and J. Ferber, Prog. Photovoltaics, 2001, 9, 425–438 CAS .
90. J. Gao, M. B. Achari and L. Kloo, Chem. Commun., 2014, 50, 6249–6251
91. W. Yang, Y. Hao, P. Ghamgosar and G. Boschloo, Electrochim. Acta, 2016, 219, 879–886 CrossRef CAS.
92. B. Li, L. Wang, B. Kang, P. Wang and Y. Qiu, Sol. Energy Mater. Sol. Cells, 2006, 90, 549–573 CrossRef CAS
93. J.-H. Yum, P. Chen, M. Grätzel and M. K. Nazeeruddin, ChemSusChem, 2008, 1, 699–707 CrossRef CAS PubMed .

96. J. Zhang, N. Vlachopoulos, M. Jouini, M. B. Johansson, X. Zhang, M. K. Nazeeruddin, G. Boschloo, E. M. J. Johansson and A. Hagfeldt, Nano Energy, 2016, **19**, 455–470 CrossRef CAS
97. Nick84, Spectrum of Solar Radiation (Earth), 14 February 2013. URL: https://commons.wikimedia.org/wiki/File:Solar_spectrum_en.svg.
98. G. Nofuentes, B. García-Domingo, J. V. Muñoz and F. Chenlo, Appl. Energy, 2014, **113**, 302–309 CrossRef CAS
99. C. A. Gueymard, D. Myers and K. Emery, Sol. Energy, 2002, **73**, 443–467 CrossRef
100. C. A. Gueymard, Sol. Energy, 2004, **76**, 423–453 CrossRef
101. J. F. Randall and J. Jacot, Renewable Energy, 2003, **28**, 1851–1864 CrossRef CAS
102. N. Tanabe, Fujikura Tech. Rev., 2013, **42**, 109–113 Search PubMed
103. F. De Rossi, T. Pontecorvo and T. M. Brown, Appl. Energy, 2015, **156**, 413–422 CrossRef
104. I. Mathews, P. J. King, F. Stafford and R. Frizzell, IEEE J. Photovolt., 2016, **6**, 230–235 Search PubMed
105. I. Mathews, S. N. Kantareddy, T. Buonassisi and I. M. Peters, Joule, 2019, **3**, 1415–1426 CrossRef CAS
106. H. Michaels, I. Benesperi and M. Freitag, Chem. Sci., 2021, **12**, 5002–5015 **RSC**
107. Yun, Sining, Yong Qin, Alexander R. Uhl, Nick Vlachopoulos, Min Yin, Dongdong Li, Xiaogang Han, and Anders Hagfeldt. "New-generation integrated devices based on dye-sensitized and perovskite solar cells." Energy & Environmental Science 11, no. 3 (2018): 476-526.
108. Roose, B., Pathak, S. and Steiner, U., 2015. Doping of TiO 2 for sensitized solar cells. Chemical Society Reviews, 44(22), pp.8326-8349.
109. Yeoh, M.E. and Chan, K.Y., 2017. Recent advances in photo-anode for dye-sensitized solar cells: a review. International Journal of Energy Research, 41(15), pp.2446-2467.
110. Narayan, M.R., 2012. Dye sensitized solar cells based on natural photosensitizers. Renewable and sustainable energy reviews, 16(1), pp.208-215.
111. Syed, T.H. and Wei, W., 2022. Technoeconomic Analysis of Dye Sensitized Solar Cells (DSSCs) with WS2/Carbon Composite as Counter Electrode Material. Inorganics, 10(11), p.191.
112. Dye Sensitized Solar Cells-Dye Solar Cells-DSSC-DSC Gamry Instruments

113. ASTM Standard E948–16, Test Method for Electrical Performance of Photovoltaic Cells Using Reference Cells Under Simulated Sunlight, ASTM International technical report, 2020.
114. Takagi, S. Magaino, H. Saito, T. Aoki and D. Aoki, J. Photochem. Photobiol., C, 2013, **14**, 1–12 CrossRef CAS
115. N. Koide and L. Han, Rev. Sci. Instrum., 2004, **75**, 2828–2831 CrossRef CAS
116. R. Jiang and G. Boschloo, J. Mater. Chem. A, 2018, **6**, 10264–10276 **RSC**
117. H. J. Snaith, *Nat. Photonics*, 2012, **6**, 337–340 CrossRef CAS
118. https://www.sciencedirect.com/topics/materials-science/x-ray-diffraction-analysis
119. https://microbenotes.com/scanning-electron-microscope-sem/
120. https://serc.carleton.edu/research_education/geochemsheets/techniques/SEM.html
121. https://chem.libretexts.org/Bookshelves/
Physical_and_Theoretical_Chemistry_Textbook_Maps/
Supplemental_Modules_(Physical_and_Theoretical_Chemistry)/Kinetics/02%
3A_Reaction_Rates/2.01%3A_Experimental_Determination_of_Kinetics/2.1.05%
3A_Spectrophotometry#:~:text
122. Fundamentals of Spectrophotometry, W.H.Freeman and Company